The Plant Cell, Vol. 29: 2233–2248, September 2017, www.plantcell.org © 2017 ASPB.

GENERAL CONTROL NONREPRESSIBLE4 Degrades 14-3-3 and the RIN4 Complex to Regulate Stomatal Aperture with Implications on Nonhost Disease Resistance and Drought Tolerance[OPEN]

Amita Kaundal,[1,2] Vemanna S. Ramu,[1] Sunhee Oh, Seonghee Lee,[3] Bikram Pant, Hee-Kyung Lee, Clemencia M. Rojas,[4] Muthappa Senthil-Kumar,[5] and Kirankumar S. Mysore[6]

Noble Research Institute, Ardmore, Oklahoma 73401

ORCID IDs: 0000-0002-9154-1173 (A.K.); 0000-0002-9729-8768 (V.S.R.); 0000-0002-5190-8014 (S.L.); 0000-0002-8690-1832 (B.P.); 0000-0003-1502-1659 (M.S.-K.); 0000-0002-9805-5741 (K.S.M.)

Plants have complex and adaptive innate immune responses against pathogen infections. Stomata are key entry points for many plant pathogens. Both pathogens and plants regulate stomatal aperture for pathogen entry and defense, respectively. Not all plant proteins involved in stomatal aperture regulation have been identified. Here, we report GENERAL CONTROL NONREPRESSIBLE4 (GCN4), an AAA$^+$-ATPase family protein, as one of the key proteins regulating stomatal aperture during biotic and abiotic stress. Silencing of *GCN4* in *Nicotiana benthamiana* and *Arabidopsis thaliana* compromises host and nonhost disease resistance due to open stomata during pathogen infection. *AtGCN4* overexpression plants have reduced H$^+$-ATPase activity, stomata that are less responsive to pathogen virulence factors such as coronatine (phytotoxin produced by the bacterium *Pseudomonas syringae*) or fusicoccin (a fungal toxin produced by the fungus *Fusicoccum amygdali*), reduced pathogen entry, and enhanced drought tolerance. This study also demonstrates that AtGCN4 interacts with RIN4 and 14-3-3 proteins and suggests that GCN4 degrades RIN4 and 14-3-3 proteins via a proteasome-mediated pathway and thereby reduces the activity of the plasma membrane H$^+$-ATPase complex, thus reducing proton pump activity to close stomata.

INTRODUCTION

Plants are exposed to a variety of pathogenic microbes and therefore have a complex innate immune system (Jones and Dangl, 2006). The plant's innate immune system includes preformed physical and chemical barriers that prevent pathogen ingress as well as induced defenses triggered by pathogen-associated molecular patterns (PAMPs) or pathogen effectors that limit pathogen proliferation. Induced defenses include closure of stomata, programmed cell death at the site of infection, known as the hypersensitive response (HR), enhanced expression of defense-related genes, and the oxidative burst. Plants are resistant to most potential pathogens due to the phenomenon known as nonhost resistance (Heath, 2000). Nonhost resistance is polygenic, broad spectrum, and more durable than host resistance or *R* gene-mediated resistance, where some cultivars within a species are resistant while others are susceptible to a pathogen (Heath, 1987; Gill et al., 2015). A pathogen that has the ability to cause disease on a given plant is called a host pathogen, while a pathogen unable to cause disease in a given plant is called a nonhost pathogen (Mysore and Ryu, 2004; Senthil-Kumar and Mysore, 2013). Few *Pseudomonas syringae* strains do not infect *Arabidopsis thaliana* and are considered as nonhost mainly because they lack two genes that are required to detoxify the *Brassica*-specific defense metabolites, alkyl glucosinolates (Fan et al., 2011). These compounds control stomatal aperture in response to wounding in Arabidopsis (Zhao et al., 2008) and are linked to altered drought response in *Brassica* species (Del Carmen Martínez-Ballesta et al., 2013).

Many pathogens infect plants by entering through stomata or wounds (Melotto et al., 2006). Stomatal closure is an induced plant defense mechanism in response to pathogen recognition (Melotto et al., 2006). For instance, flg22, a 22-mer fragment of bacterial flagellin, is recognized by the cognate pathogen recognition receptor FLS2 and induces a signal transduction cascade that closes stomata (Zeng and He, 2010). To counteract plant defense, host pathogens secrete virulence metabolites like coronatine (COR) and fusicoccin to reopen stomata (Marre, 1979; Gudesblat et al., 2009; Lee et al., 2013). Stomatal closure is also observed with the activation of MITOGEN-ACTIVATED PROTEIN KINASE3 (MAPK3; Meng and Zhang, 2013), induction of the plant defense hormone salicylic acid (Jones and Dangl, 2006), and upregulation of NONEXPRESSOR OF PATHOGENESIS-RELATED GENE1 upon salicylic acid induction (Maier et al., 2011). A rapid stomatal

[1] These authors contributed equally to this work.
[2] Current address: Department of Environmental Sciences, University of California, Riverside, CA 92521.
[3] Current address: Gulf Coast Research and Education Center, University of Florida, Wimauma, FL 33598.
[4] Current address: Department of Plant Pathology, University of Arkansas, Fayetteville, AR 72701.
[5] Current address: National Institute of Plant Genome Research, New Delhi, India.
[6] Address correspondence to ksmysore@noble.org.
The author responsible for distribution of materials integral to the findings presented in this article in accordance with the policy described in the Instructions for Authors (www.plantcell.org) is: Kirankumar S. Mysore (ksmysore@noble.org).
[OPEN]Articles can be viewed without a subscription.
www.plantcell.org/cgi/doi/10.1105/tpc.17.00070

response also occurs due to environmental stimuli such as drought, humidity, temperature, and light (Lim et al., 2015). Stomatal closure is also triggered by abscisic acid (ABA), a phytohormone that accumulates in plants during drought stress and biotic stress (Sirichandra et al., 2009b). The stomatal responses are regulated by several proteins, including respiratory burst oxidases, that are involved in both biotic and abiotic stress responses. These proteins are phosphorylated by the SnRK2 protein kinase OPEN STOMATA1 (OST1) during ABA-dependent stomatal closure (Sirichandra et al., 2009a).

The plasma membrane (PM)-localized Arabidopsis H^+-ATPases (AHA1 and AHA2) play a crucial role in PAMP-induced stomatal closure (Liu et al., 2009). These ATPases generate a transmembrane electron gradient upon activation that helps the inward flow of K^+ ions and leads to the uptake of solute and water into the guard cells. This uptake of water results in the swelling of guard cells and opening of stomata. These H^+-ATPases are constitutively active in the Arabidopsis mutant *ost2*, resulting in stomata that remain open even upon exogenous application of ABA (Merlot et al., 2007; Arnaud and Hwang, 2015). The *ost2* mutant also does not close stomata in response to bacteria and PAMPs such as flg22 and lipopolysaccharides (Liu et al., 2009). Therefore, the *ost2* mutant, when inoculated by spraying, is susceptible to *P. syringae* pv *tomato* (DC3000) expressing the

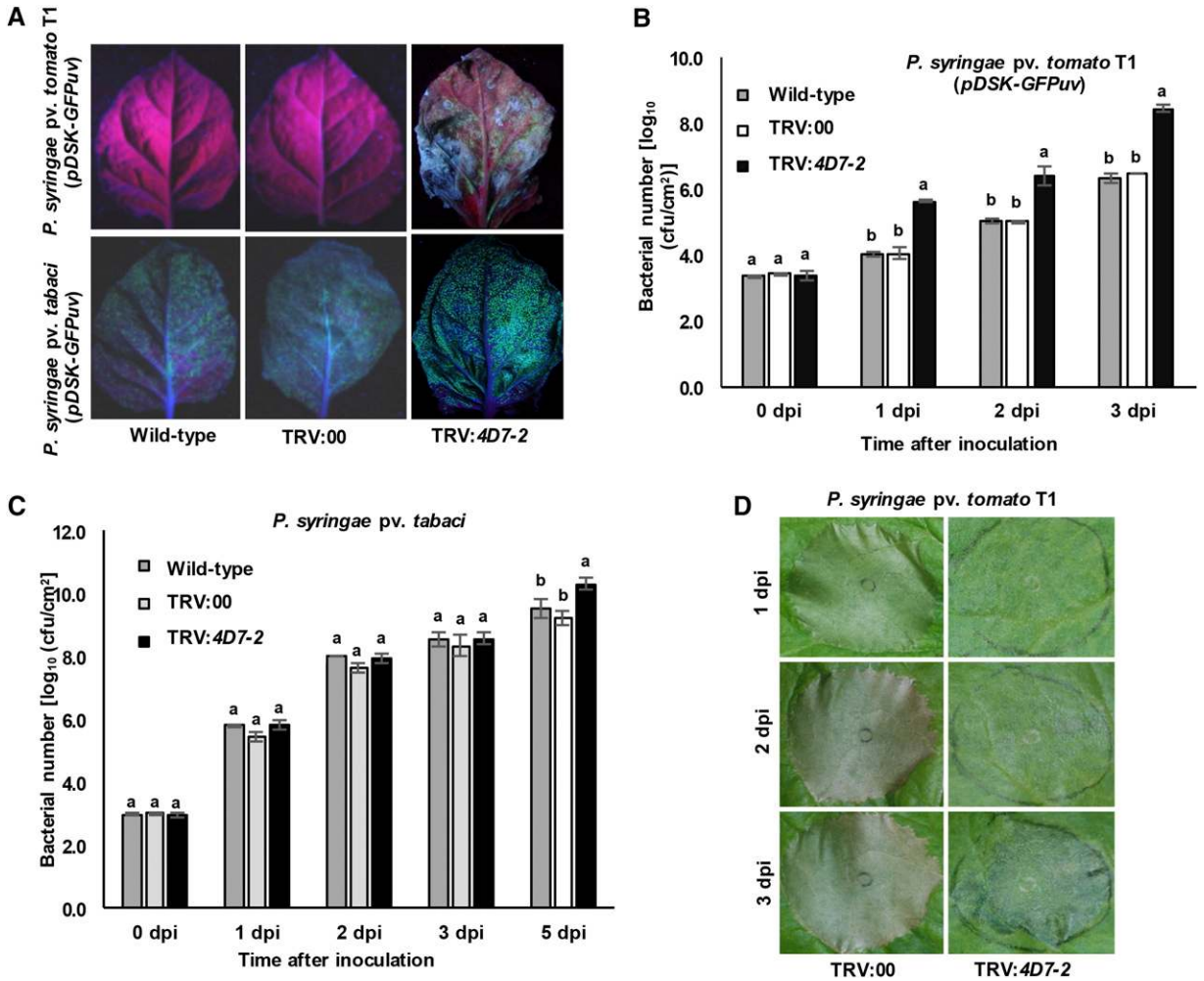

Figure 1. Silencing of the *4D7*-2 cDNA Clone in *N. benthamiana* Enhances Multiplication of Host and Nonhost Pathogens.

(A) Visualization of host and nonhost bacterial multiplication in TRV:*4D7-2*- or TRV:00-inoculated *N. benthamiana* plants. Three weeks after TRV inoculation, *N. benthamiana* plants were vacuum infiltrated with the nonhost pathogen *P. syringae* pv *tomato* T1 (*pDSK-GFPuv*) and the host pathogen *P. syringae* pv *tabaci* (*pDSK-GFPuv*) at 10^4 cfu/mL. Photographs were taken at 5 dpi under UV light.

(B) and **(C)** Quantification of nonhost **(B)** and host **(C)** bacterial multiplication in TRV:*4D7-2* and TRV:00. Leaves were syringe inoculated with nonhost or host pathogens (1×10^7 cfu/mL). Average values of three biological replicates from three individual plants were used, and experiments were repeated three times with similar results. Error bars indicate SE. Different letters above the bars indicate significant differences from two-way ANOVA at $P < 0.05$ with Tukey's HSD means separation test ($\alpha = 0.05$) within a time point.

(D) Development of the HR in response to nonhost pathogen. The abaxial side of *4D7-2*-silenced and control leaves was inoculated with *P. syringae* pv *tomato* T1 (1×10^8 cfu/mL) using a needleless syringe. HR symptoms (cell death) were documented at different dpi.

effector AvrRpt2, which induces effector-triggered immunity (Liu et al., 2009). AHA1 and AHA2 interact with RIN4 (RPM1-INTERACTING PROTEIN4), which is a well-known regulator of multiple plant immune responses (Liu et al., 2009). RIN4 has been shown to play a major role in PAMP-triggered immunity, effector-triggered immunity, and stomatal opening upon pathogen perception (Mackey et al., 2002; Liu et al., 2009). RIN4 is expressed in guard cells and interacts with AHA1 and AHA2 proteins to regulate the PM H^+-ATPase activity and thereby trigger stomatal opening and closing during PAMP-triggered immunity (Liu et al., 2009). The 14-3-3 protein is a regulatory protein that interacts with the C-terminal part of AHA1 and phosphorylates AHA2 at a serine/threonine residue, thereby activating a PM H^+-ATPase to generate a differential proton gradient across the guard cell membrane to open stomata (Jahn et al., 1997; Baunsgaard et al., 1998). The proteasome-mediated degradation of 14-3-3 proteins by the E3 ligase ATL31 has been shown to occur due to stress stimuli such as high-carbon or low-nitrogen conditions (Yasuda et al., 2014). Overexpression of *RIN4* increases the activation of H^+-ATPases, while the *rin4* mutant has reduced H^+-ATPase activity and is resistant to *P. syringae* pv *tomato* (DC3000) (Liu et al., 2009). RPM1 is a disease resistance protein that protects plants against pathogens that contain a particular avirulence protein, via an indirect interaction with RIN4, and triggers plant resistance (Lee et al., 2015). Activation of jasmonic acid (JA) signaling by the bacterial secretory protein AvrB through MAPK4-mediated phosphorylation of RIN4 in response to pathogen attack induces stomatal closure (Cui et al., 2010). The fungal pathogen of peach (*Prunus persica*), *Fusicoccum amygdali*, secretes fusicoccin, which targets the PM H^+ proton pump complex and stabilizes it by binding with 14-3-3 protein, thereby keeping the stomata open (Marre, 1979; Jahn et al., 1997; Baunsgaard et al., 1998).

Another class of ATPase proteins known as AAA (ATPases associated with diverse cellular activities)$^+$-ATPases have diverse functions, such as protein folding and unfolding, assembly or disassembly of protein complexes, and protein transport and degradation (White and Lauring, 2007; Ogura et al., 2012). Few AAA^+-ATPases are components of the core subunit (20S) and recognition complex (19S) of the 26S proteasome complex (Vierstra, 2009; Sousa, 2014). The 19S recognizes and binds to ubiquitinated proteins and unfolds substrates in an ATP-dependent manner (Kim et al., 2011). In this process, ATPase mediates the energy-dependent removal of folded and aggregated proteins by acting as a chaperone that unfolds and disaggregates protein substrates (Sousa, 2014). The Arabidopsis protein encoded by

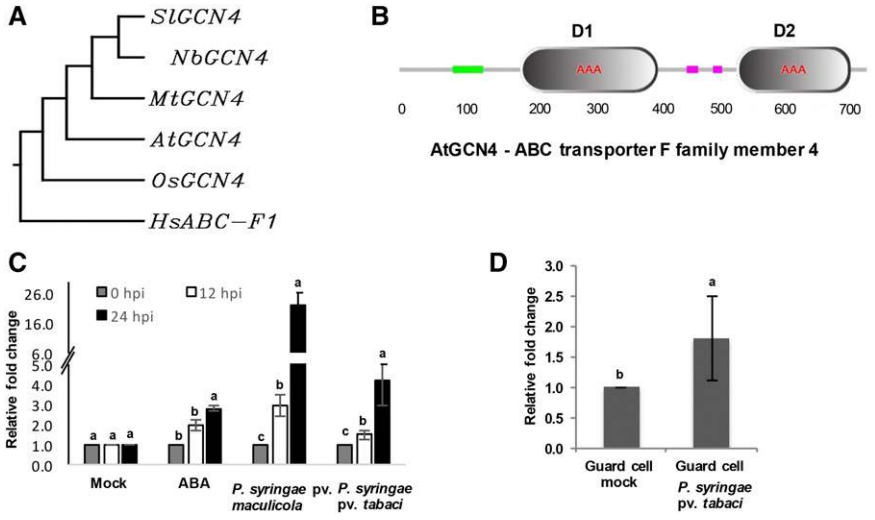

Figure 2. GCN4 Is Conserved and Induced under ABA and Pathogen Stress.

(A) Phylogenetic map of GCN4 orthologs by nearest neighbor analysis using the geneious tool. Alignments used to generate the phylogeny are provided in Supplemental Data Set 1.

(B) Protein map of AtGCN4 showing the two AAA domains (D1 and D2) predicted by the Simple Modular Architecture Research Tool (http://smart.embl-heidelberg.de/).

(C) *AtGCN4* transcript analyses in ABA- or pathogen-treated wild-type Arabidopsis plants. The expression of *AtGCN4* is shown in response to ABA, the host bacterium *P. syringae* pv *maculicola*, and the nonhost bacterium *P. syringae* pv *tabaci* at 0, 12, and 24 hpi. Three-week-old Col-0 Arabidopsis plants were treated with 10 μM ABA or *P. syringae* pv *maculicola* or *P. syringae* pv *tabaci* at 10^5 cfu/mL. Mature leaves from a minimum of three biological replicates representing three individual plants were used to assess the expression of *GCN4* in each treatment. Different letters above the bars indicate significant differences from two-way ANOVA at $P < 0.05$ with Tukey's HSD means separation test ($\alpha = 0.05$) within a time point.

(D) Expression of *AtGCN4* in guard cell-specific tissue as quantified by RT-qPCR. Wild-type Arabidopsis Col-0 plants were inoculated with *P. syringae* pv *tabaci* (4×10^7 cfu/mL) by spray inoculation along with a mock control. Leaf tissue was collected at 24 hpi, and guard cells were enriched. RNA from the guard cell-enriched samples was analyzed by RT-qPCR. Error bars represent SE from three biological replicates representing three individual plants. Different letters above the bars indicate significant differences from two-way ANOVA between mock and treatment at $P < 0.05$ with Tukey's HSD means separation test ($\alpha = 0.05$).

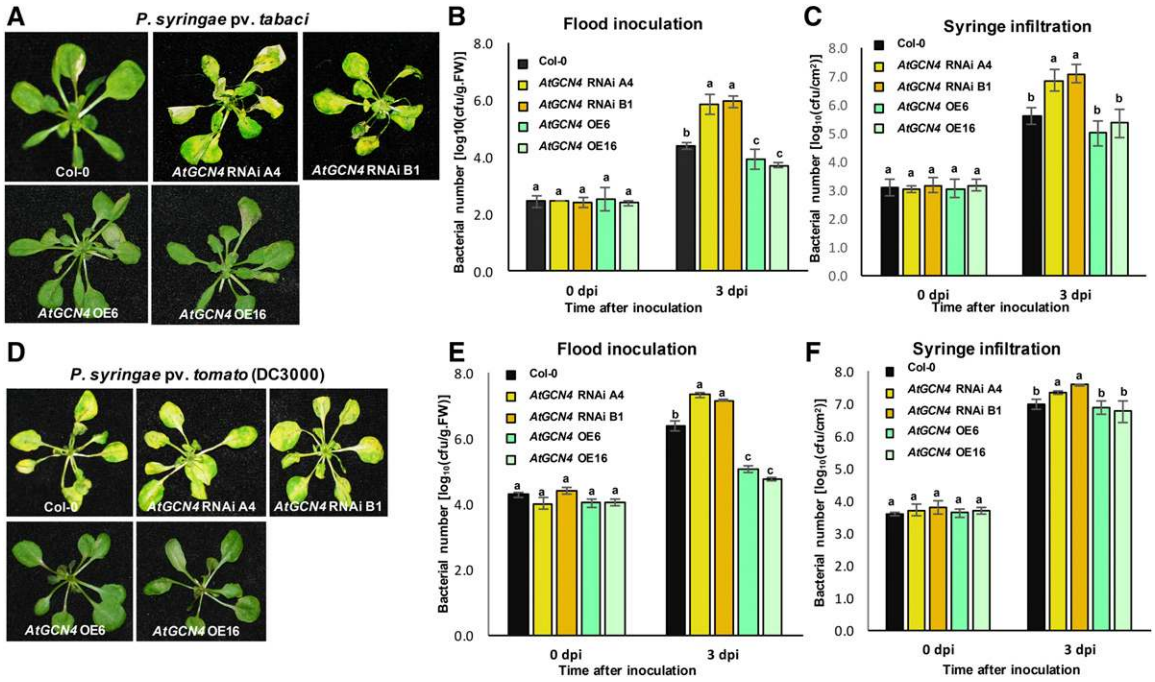

Figure 3. *AtGCN4* RNAi Plants Compromise Nonhost Disease Resistance, and Overexpression Plants Show Tolerance to Host Pathogen.

(A) Arabidopsis *GCN4* RNAi lines showed compromised resistance to the nonhost pathogen *P. syringae* pv *tabaci* (1×10^5 cfu/mL) when inoculated by flooding.

(B) Bacterial titer was assessed at 0 and 3 dpi in leaves of seedlings that were flood inoculated with *P. syringae* pv *tabaci*.

(C) Bacterial titer was also assessed when inoculated by syringe infiltration with *P. syringae* pv *tabaci* (1×10^4 cfu/mL).

(D) Phenotypic responses of Arabidopsis lines treated with the host pathogen *P. syringae* pv *tomato* (DC3000) by flood inoculation (1×10^5 cfu/mL).

(E) Bacterial titer was assessed at 0 and 3 dpi in leaves of seedlings that were flood inoculated with DC3000.

(F) Bacterial titer was also assessed when inoculated by syringe infiltration with the host pathogen DC3000 (1×10^4 cfu/mL).

Error bars represent SE for three biological replicates representing three individual plants in three independent experiments. Different letters above the bars indicate significant differences from two-way ANOVA at $P < 0.05$ with Tukey's HSD means separation test ($\alpha = 0.05$) within a time point. FW, fresh weight.

AIA1 (ABA-induced AAA$^+$-ATPase) acts as a chaperone and is regulated by *ABSCISIC ACID-RESPONSIVE ELEMENT BINDING PROTEIN1* (*AREB1*; Fujita et al., 2005). Plants overexpressing *AREB1* showed improved drought tolerance (Fujita et al., 2005).

Here, we identified GENERAL CONTROL NONREPRESSIBLE4 (GCN4), a AAA$^+$-ATPase, as a novel player in stomatal aperture regulation and thus in plant innate immunity and drought tolerance. We show that GCN4 interacts with RIN4 and 14-3-3 proteins and when overexpressed reduces PM H$^+$-ATPase activity, resulting in stomatal closure during pathogen infection.

RESULTS

Silencing of the *4D7-2* cDNA Clone in *Nicotiana benthamiana* Compromises Nonhost Resistance

To identify genes involved in nonhost disease resistance mechanisms, we conducted virus-induced gene silencing (VIGS) (Senthil-Kumar and Mysore, 2014)-based forward genetic screens in *N. benthamiana* (Rojas et al., 2012) and identified the *4D7-2* cDNA clone (NbME04D07-2) that compromises nonhost disease resistance when silenced (Figure 1A). VIGS caused stunted growth and thick curled leaves with 85% downregulation of *4D7-2* transcripts (Supplemental Figures 1A and 1B). The silenced plants showed 10-fold higher bacterial multiplication of nonhost *P. syringae* pv *tomato* T1 expressing green fluorescence protein uv (GFPuv) (Wang et al., 2007) than in wild-type or non-silenced control (TRV:00) plants (Figure 1B). Nonhost pathogens such as *P. syringae* pv *glycinea* and *Xanthomonas campestris* pv *vesicatoria* also caused disease symptoms with necrosis and chlorosis and increased bacterial multiplication in *4D7-2*-silenced plants (Supplemental Figure 1C). The bacterial titer of the host pathogen *P. syringae* pv *tabaci* (*GFPuv*) was also slightly higher (~1.5-fold) in *4D7-2*-silenced plants in comparison with non-silenced control plants at 5 days postinoculation (dpi) (Figure 1C). Infiltration with a higher concentration (1×10^4 cfu/mL) of nonhost pathogens, *P. syringae* pv *tomato* T1 (Figure 1D) or *P. syringae* pv *maculicola* (Supplemental Figure 1d), showed a delayed HR at 1, 2, and 3 dpi in *4D7-2*-silenced plants when compared with control plants. These results suggest that silencing of *4D7-2* compromises defense responses in *N. benthamiana* plants.

A nucleotide BLAST analysis of the *Nb4D7-2* sequence showed 98 and 95% homology with *Nicotiana tomentosiformis* (LOC104098889) and *Solanum tuberosum* (LOC102578605) ABC transporter F family member 4-like mRNA, respectively. The amino

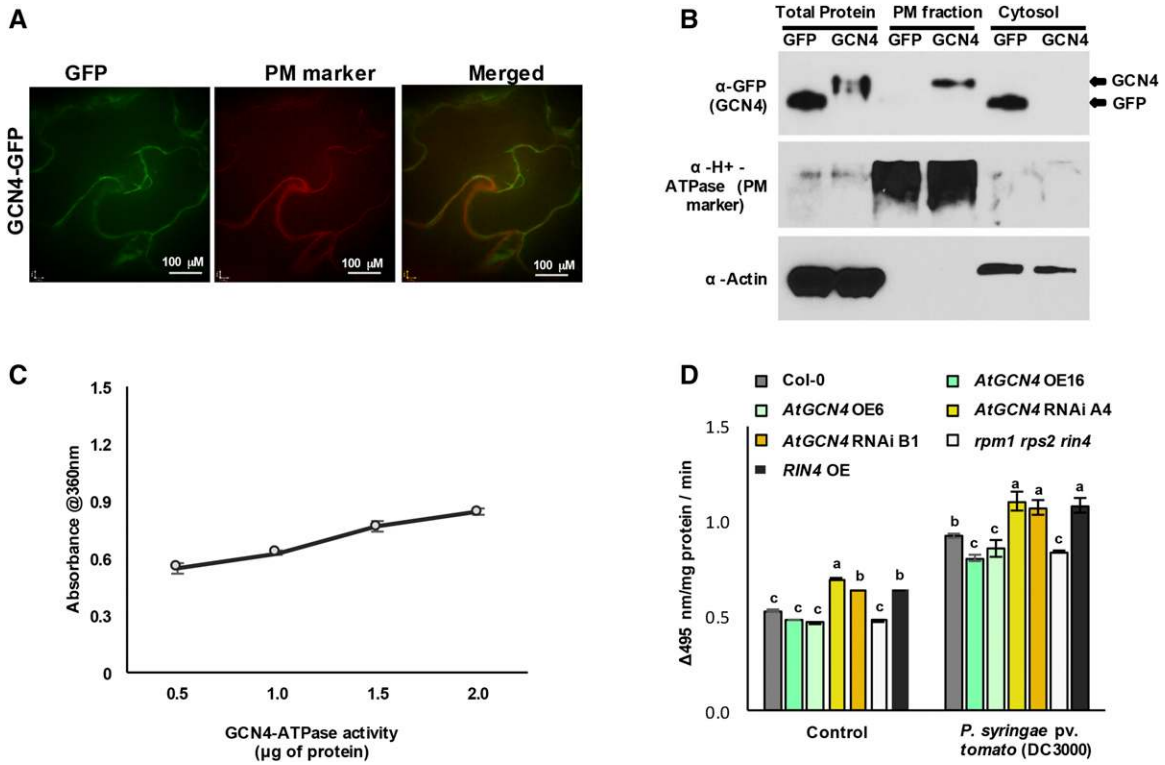

Figure 4. GCN4 Localizes to the PM and Regulates PM H+-ATPase Activity.

(A) Native promoter-driven *AtGCN4-GFP* expression localized to the PM. The PM dye FM4-64 was used as a marker. Leaves from 3-week-old stable Arabidopsis transgenic plants expressing *AtGCN4-GFP* were observed by spinning disk confocal microscopy. Over 50 images were analyzed, and a representative image is shown. Bars = 100 μm.

(B) Membrane fractions showing AtGCN4 enrichment in the PM. The PM and cytosolic fraction proteins were extracted from Arabidopsis transgenic lines expressing *AtGCN4-GFP* (GCN4) or *GFP-GUS* (GFP). Enrichment of GCN4 and GFP in the PM and cytosolic fractions was determined by immunoblotting with GFP antiserum. H+-ATPase and Actin were used as the PM marker and loading control, respectively.

(C) GCN4 has ATPase activity. ATPase activity of GCN4 was assayed on the substrate 2-amino-6-mercapto-7-methylpurine riboside, and Pi released from the enzymatic reactions was quantified. The recombinant His tag-fused GCN4 was purified with the Ni-NTA column, and eluate was used to assess the enzyme activity.

(D) PM H+-ATPase activity increased in all the tested lines upon treatment with the host pathogen *P. syringae* pv *tomato* (DC3000) compared with control conditions. Leaf tissue was harvested 48 h posttreatment, and PMs were immediately purified. PM H+-ATPase enzymatic activity was determined from the inside-out PM vesicles from the *AtGCN4* overexpression lines, *AtGCN4* RNAi lines, *RIN4* overexpression line, and *rpm1 rps2 rin4* mutant line under control and pathogen-treated conditions. *RIN4* lines were sprayed with dexamethasone (20 mM), while Col-0, *AtGCN4* overexpression, and RNAi lines were sprayed with water containing 0.025% Silwet as a control. ATP hydrolysis and pumping of H+ ions into vesicles by H+-ATPase were measured using the pH probe acridine orange at Δ495 nm/mg protein/min. The PM proton pump activity was measured from two independent experiments with three biological replicates representing three individual plants from each genotype. Different letters above the bars indicate significant differences from two-way ANOVA at $P < 0.05$ with Tukey's HSD means separation test ($\alpha = 0.05$).

acid BLAST analysis showed 80% homology with GCN4 (ATP BINDING CASSETTE F4 family) of Arabidopsis, 94% homology with tomato (*Solanum lycopersicum*) ABC transporter-like protein, 86% with rice (*Oryza sativa*) ABC transporter-like protein, 82% with *Medicago truncatula* ABC transporter-like protein, and 46% with *Homo sapiens* ABC-F1 protein. The phylogenetic analysis suggests that GCN4 from tomato has close homology with GCN4 of *N. benthamiana* (Figure 2A; Supplemental Data Set 1). Protein analysis of AtGCN4 using the Simple Modular Architecture Research Tool showed the presence of two AAA domains from amino acid positions 187 to 400 (AAAD1) and 522 to 698 (AAAD2) (Figure 2B). There are five major clades of AAA proteins, including the Clp family, proteasome subunits, metalloproteases, ATPases with two AAA domains, and the MSP1/katanin/spastin group (White and Lauring, 2007). Since AtGCN4 has two AAA domains, it belongs to the ATPase clade.

AtGCN4 Plays an Active Role in Plant Immunity against Bacterial Pathogens in Arabidopsis

To determine the role of AtGCN4 in plant immunity and its role in regulating stomata, *AtGCN4* expression in response to ABA (a regulator of stomatal opening) or pathogen treatments in Arabidopsis Col-0 plants was assessed. A 3-fold increased expression of *AtGCN4* with response to ABA was observed. Expression was also induced at 12 and 24 hours postinoculation (hpi) in response to the host pathogen *P. syringae* pv *maculicola* and the nonhost pathogen *P. syringae* pv *tabaci* (Figure 2C). Induction of *GCN4* in

guard cells in response to nonhost pathogen was measured by isolating guard cells from *P. syringae* pv *tabaci*-treated wild-type Arabidopsis plants. *AtGCN4* was slightly induced in guard cells in response to *P. syringae* pv *tabaci* (Figure 2D). These results suggest that GCN4 may play an active role in plant defense mediated through stomata regulation.

For functional characterization of *AtGCN4*, Arabidopsis RNAi and overexpression lines were developed (Supplemental Figures 2A and 2B). *Atgcn4* knockout mutants were not available in any of the publicly available Arabidopsis mutant collections, suggesting that complete loss of *AtGCN4* may lead to lethality. RNAi lines had smaller and overexpression plants had slightly larger rosette areas and diameters compared with wild-type plants (Col-0; Supplemental Figure 2A). RNAi, overexpression, and wild-type plants were challenged with the nonhost pathogen *P. syringae* pv *tabaci* by flood inoculation (Ishiga et al., 2011). *AtGCN4* RNAi lines exhibited compromised resistance to nonhost bacteria, as they had higher levels of bacterial multiplication than the wild-type and overexpression lines (Figures 3A and 3B). This phenotypic effect was confirmed by syringe infiltration, which introduces bacteria directly into the apoplast, bypassing the entry of bacteria through stomata. Interestingly, even though the RNAi lines supported more bacterial multiplication than Col-0, the increase in bacterial number in RNAi lines was less with syringe infiltration than with flood inoculation (Figure 3C).

When flood-inoculated with the host pathogen *P. syringae* pv *tomato* (DC3000), both Col-0 and *AtGCN4* RNAi lines showed disease symptoms (Figure 3D). RNAi lines had significantly higher bacterial titer after 3 dpi when compared with Col-0 (Figure 3E). By contrast, *AtGCN4* overexpression lines did not show any disease symptoms, and the bacterial titer was dramatically less (~100-fold) after 3 dpi when compared with Col-0 (Figure 3E). Strikingly, when challenged by the host pathogen *P. syringae* pv *tomato* (DC3000) through syringe infiltration, the difference in bacterial titer between *AtGCN4* overexpression lines and Col-0 was not significant (Figure 3F). These results were consistent with those obtained in another inoculation with the host pathogen *P. syringae* pv *maculicola* (Supplemental Figure 3). These data suggest that resistance of the *AtGCN4* overexpression lines to host pathogens can occur only when the bacteria enter through natural openings such as stomata. By contrast, *AtGCN4* RNAi lines are susceptible to infection when the bacteria enter the plant through stomata or when they are directly introduced into the apoplast. However, the bacterial titer in *AtGCN4* RNAi lines was higher when bacteria entered through stomata (Figures 3B and 3E). These data suggest that *AtGCN4* has a dual role in plant defense, one through stomata-mediated immunity and the other through apoplastic defense.

AtGCN4 Is an ATPase That Regulates PM H^+-ATPase Activity

To study the subcellular localization of AtGCN4, Arabidopsis transgenic lines expressing native promoter-driven *AtGCN4-GFP* were developed. In these lines, GFP fluorescence was mainly localized in the PM (Figure 4A). To further confirm the PM localization of GCN4, PM- and cytosol-associated proteins were isolated from *AtGCN4-GFP*-expressing Arabidopsis plants. AtGCN4-GFP protein was clearly associated with the PM fraction when compared with the cytosol fraction (Figure 4B). Localization was also observed in guard cells (Supplemental Figure 4A). To study the tissue-specific expression of *AtGCN4*, Arabidopsis transgenic lines expressing *AtGCN4 Promoter-GUS* were developed. X-gluc staining for GUS activity suggested that *AtGCN4* is expressed in most parts of the plant, including leaves, flowers, roots, and stomata (Supplemental Figure 4B). Overexpression or downregulation of *AtGCN4* in Arabidopsis did not affect the development of stomata (Supplemental Figure 5).

GCN4 has conserved Walker A and Walker B domains that bind to and hydrolyze ATP, respectively, to generate a mechanical force that can be used to unfold substrate proteins (Hanson and Whiteheart, 2005). To determine the ATPase activity of AtGCN4 that may be involved in energy-mediated substrate degradation, the recombinant protein (Supplemental Figure 6) was assayed on the substrate 2-amino-6-mercapto-7-methylpurine riboside and the Pi content in solution was quantified. The increased Pi release with the increasing concentration of GCN4 protein confirms increased ATPase activity (Figure 4C).

Further, as AtGCN4 was localized to the PM, we assessed PM H^+-ATPase activity in *AtGCN4* overexpression and RNAi lines. The PM-enriched vesicles were isolated from 5-week-old Col-0, *AtGCN4* RNAi, and overexpression lines and the H^+-ATPase activity was measured as described (Liu et al., 2009). *AtGCN4* RNAi lines had increased PM H^+-ATPase activity compared with wild-type Col-0 (Figure 4D). *AtGCN4* overexpression lines showed slightly lower PM H^+-ATPase activity compared with Col-0 (Figure 4D). Interestingly, after pathogen treatment, the PM H^+-ATPase activity was higher than in untreated samples in all the lines tested (Figure 4D). Similar to that of untreated samples, the PM H^+-ATPase activity was significantly lower in *AtGCN4*-overexpressing plants and higher in RNAi lines when compared with Col-0 upon treatment with host pathogen (Figure 4D). These results indicate that GCN4 has ATPase activity and hence that energy-mediated disassembly of the PM H^+-ATPase complex by GCN4 is possible. *RIN4* overexpressor and mutant lines were used as experimental checks, since RIN4 has been previously shown to regulate PM H^+-ATPase (Liu et al., 2009). *RIN4* overexpression lines showed enhanced PM H^+-ATPase activity, whereas the *rpm1 rps2 rin4* triple mutant showed decreased activity than Col-0 (Figure 4D), which is consistent with previously reported results (Liu et al., 2009). Further, similar to an earlier report (Liu et al., 2009), the *rpm1 rps2 rin4* mutant line showed tolerance to the host pathogen *P. syringae* pv *tomato* (DC3000) (Figures 5A and 5B). Interestingly, *AtRIN4* overexpression lines showed compromised nonhost resistance both by flood (Figures 5C and 5D) and spray (Figures 5E and 5F) methods of inoculation. Taken together, these data suggest that GCN4 and RIN4 regulate the activity of PM H^+-ATPases that influence the ability of pathogens to enter the apoplast.

AtGCN4 Regulates Stomatal Aperture in Response to Various Treatments

Dependence on stomata-based bacterial entry to confer disease resistance in *AtGCN4* overexpression lines, *AtGCN4* expression in guard cells, and the ability of GCN4 to regulate PM H^+-ATPase suggested that *GCN4* was involved in stomatal aperture regulation. Therefore, stomatal aperture was measured in *AtGCN4* overexpression and RNAi lines that were treated with compounds

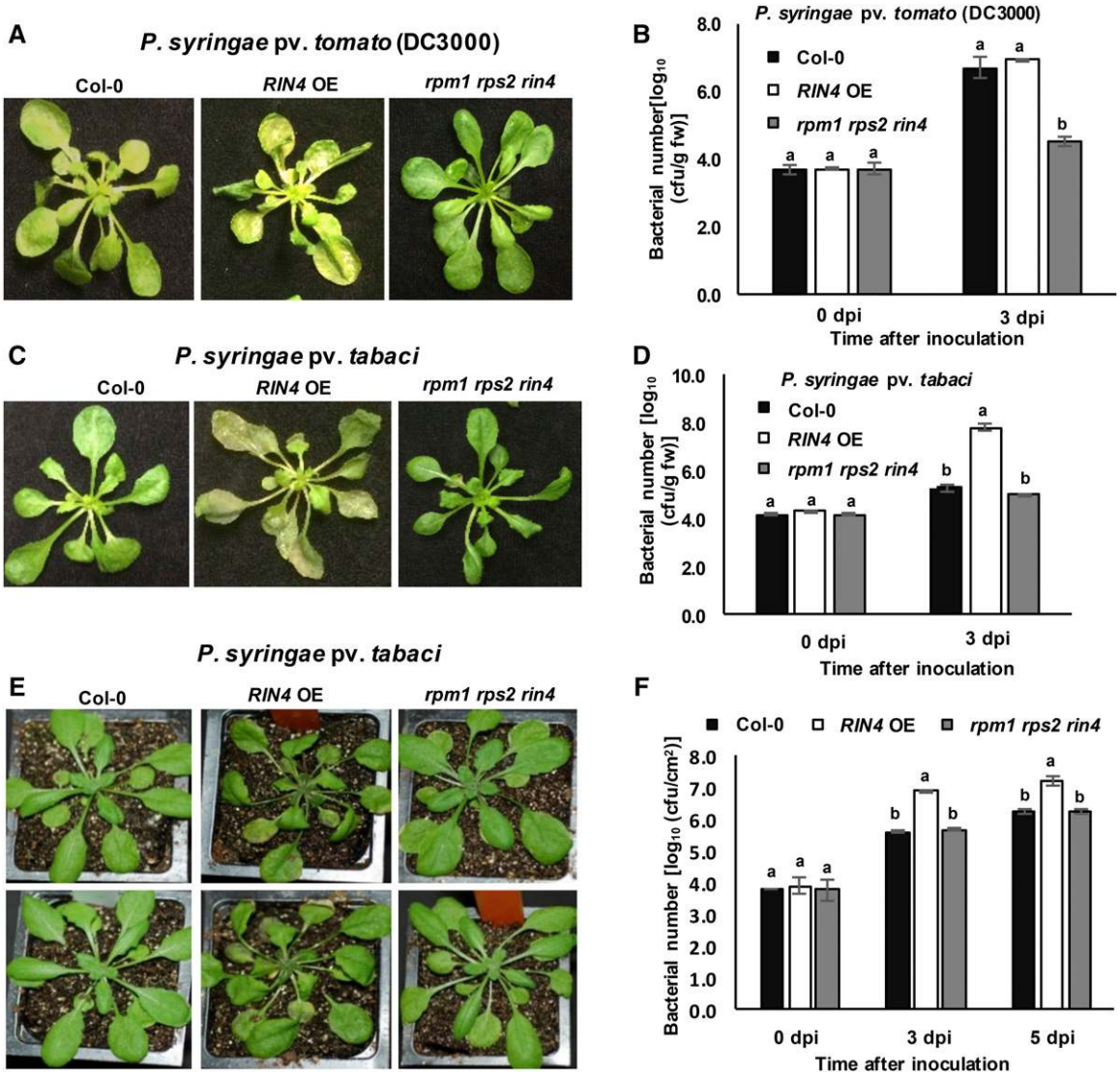

Figure 5. Overexpression of *RIN4* in Arabidopsis Plants Shows Compromised Disease Resistance to the Nonhost Pathogen *P. syringae* pv *tabaci*.

(A) The Col-0 and *RIN4* overexpression (OE) lines are susceptible and the *rpm1 rps2 rin4* mutant line is resistant to the host pathogen *P. syringae* pv *tomato* (DC3000) when infected through flood inoculation.

(B) Bacterial quantification assay confirmed the resistance of the *rpm1 rps2 rin4* mutant line.

(C) Following infection with the nonhost pathogen *P. syringae* pv *tabaci* by flood inoculation (2×10^6 cfu/mL), the *RIN4* overexpression lines were more susceptible than the mutant.

(D) Bacterial quantification assay further confirmed that *RIN4* overexpression compromises nonhost resistance.

(E) The *RIN4* overexpression plants also exhibited compromised resistance to the nonhost pathogen *P. syringae* pv *tabaci* inoculated by spraying.

(F) The *RIN4* overexpression lines harbored more bacteria than did Col-0 at 3 and 5 dpi by spraying.

Error bars represent SE from three biological replicates representing three individual plants. Different letters represent statistical significance ($P < 0.05$, two-way ANOVA). fw, fresh weight.

that can open or close stomata, such as COR, fusicoccin, and ABA (Marre, 1979; Baunsgaard et al., 1998; McLachlan et al., 2014). Treatment with COR or fusicoccin caused an open stomata phenotype in Col-0, *AtGCN4* overexpression, and RNAi lines (Figure 6A; Supplemental Figure 7A). By contrast, exogenous application of ABA closed the stomata in Col-0 and *AtGCN4* overexpression lines. However, in RNAi lines, stomata remained open upon ABA treatment (Figure 6A; Supplemental Figure 7A). Further, treatment of ABA-induced closed stomata of Col-0 with COR or fusicoccin was able to reopen stomata. Strikingly, in *AtGNC4* overexpression lines, closed stomata induced by ABA were not able to reopen in response to COR or fusicoccin treatments (Figure 6A; Supplemental Figure 7A). In addition, the stomatal apertures of overexpression lines in response to the host pathogen *P. syringae* pv *tomato* (DC3000) were significantly smaller compared with *AtGNC4* RNAi and Col-0 after 2 hpi (Figure

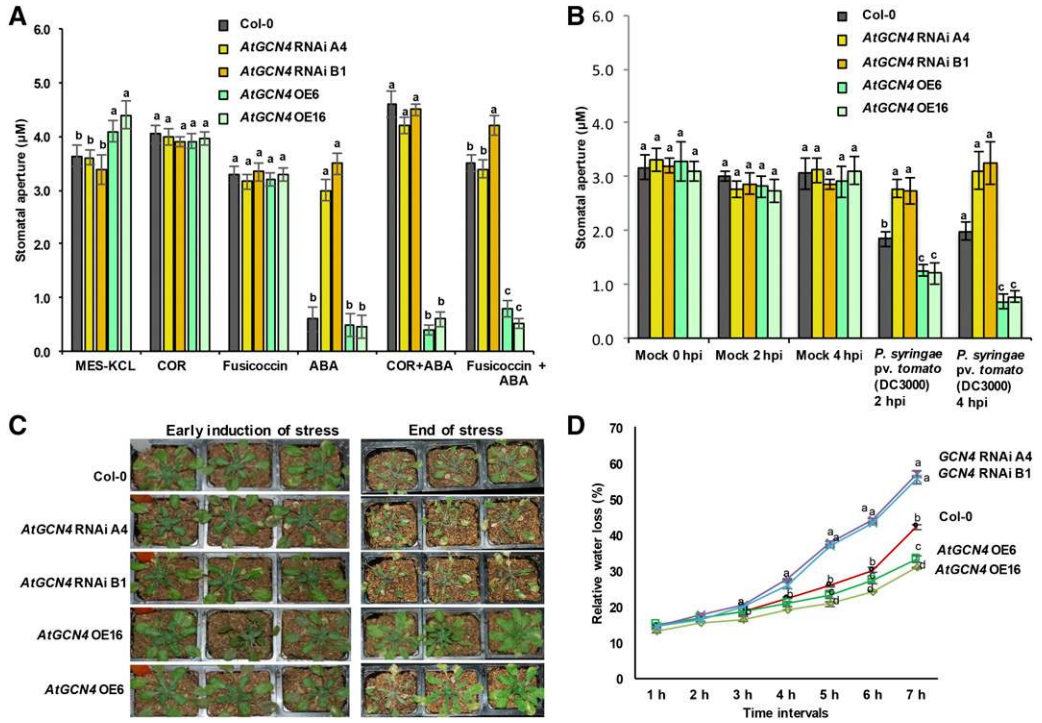

Figure 6. *AtGCN4* Regulates Stomatal Aperture and Functions in Biotic and Abiotic Stress Tolerance.

(A) Stomatal aperture size was measured at 4 h posttreatment with MES buffer, COR, fusicoccin, ABA, COR + ABA, and fusicoccin + ABA. Microscopy images were taken at 3 h posttreatment.

(B) Stomatal aperture size was measured at 2 and 4 hpi with the host pathogen *P. syringae* pv *tomato* (DC3000) (1×10^8 cfu/mL) and a mock control.

(C) AtGCN4-overexpressing Arabidopsis plants were tolerant to drought stress when exposed to gradual moisture stress for 9 d.

(D) *AtGCN4* RNAi lines lost water quickly and the overexpression lines lost water more slowly when compared with wild-type Col-0. The detached leaves of Col-0, *AtGCN4* overexpressor, and RNAi lines were air dried, and the weight of the tissue was recorded every hour.

Error bars represent SE for three biological replicates representing three individual plants. Different letters above the bars indicate significant differences from two-way ANOVA at $P < 0.05$ with Tukey's HSD means separation test ($\alpha = 0.05$) within a treatment or time point.

6B). By contrast, the stomatal aperture in RNAi lines was significantly larger than that of Col-0. Similar results were observed in response to the nonhost pathogen *P. syringae* pv *tabaci* for the RNAi lines, but the overexpression lines did not show a significant difference compared with Col-0 (Supplemental Figure 7B).

Consistent with the *AtGNC4* RNAi lines, *NbGCN4*-silenced *N. benthamiana* plants infected with the nonhost pathogen *P. syringae* pv *tomato* T1 also showed open stomata at 2 hpi (Supplemental Figure 8). As expected, the nonsilenced control plants (TRV:00) showed closed stomata due to active defense. These data suggest that GCN4 plays an important role in regulating stomatal aperture in response to biotic and abiotic stimuli.

AtGCN4 Overexpression Lines Are Drought Tolerant Compared with the Wild Type

The inability of stomata in ABA-treated *AtGCN4* overexpression lines to reopen in response to COR or fusicoccin treatment prompted us to test whether these lines confer drought tolerance. Upon imposing drought stress, *AtGCN4* RNAi and Col-0 lines showed a severe drought-sensitive phenotype with wilted leaves, while the *AtGCN4* overexpression lines remained green (Figures 6C and 6D). The *AtGCN4* RNAi lines showed more wilting symptoms than Col-0. After rewatering for 10 d, the Col-0 and RNAi lines did not survive, while the overexpression lines had a 100% survival rate with a normal phenotype upon recovery. During moisture stress, transpirational water loss through the stomata is an important factor associated with drought tolerance mechanisms. The detached rosette leaves from *AtGCN4* overexpression lines showed significantly less water loss than did those of Col-0 and RNAi plants (Figure 6D). These data suggest that *AtGCN4* overexpression leads to less stomatal water loss and hence provides drought tolerance.

GCN4 Interacts with RIN4 and 14-3-3 Proteins in Planta

The findings that GCN4 regulates stomatal aperture and mediates a decrease in PM H^+-ATPase activity upon pathogen inoculation in *AtGCN4* overexpression lines prompted us to speculate that GCN4 may disassemble PM H^+-ATPase complex-associated proteins such as RIN4, 14-3-3, AHA1, and AHA2. A protein-protein interaction study using the yeast two-hybrid (Y2H) system showed that AtGCN4 interacted with AtRIN4 and At14-3-3 proteins but not with AHA1 and AHA2 proteins (Figure 7A). Truncated GCN4

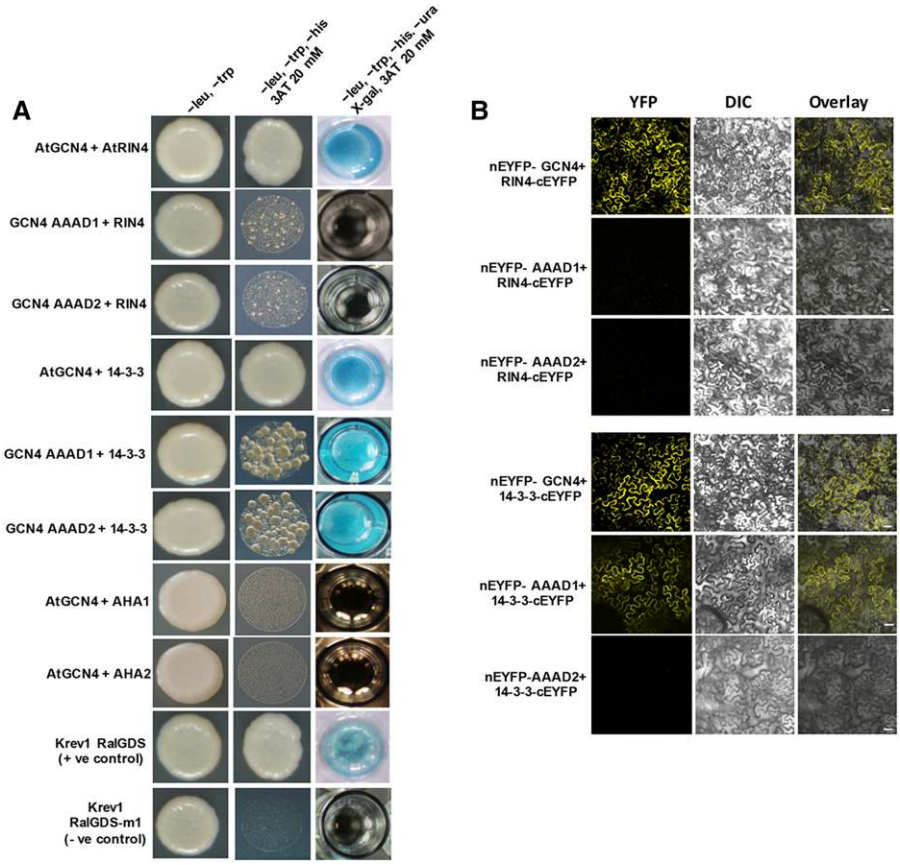

Figure 7. GCN4 Interacts with RIN4 and 14-3-3.

(A) AtGCN4 interacts with RIN4 and 14-3-3 proteins in a Y2H assay. *AtGCN4* was cloned as bait in *pDEST32* and *AtRIN4*, *At14-3-3*, *AtAHA1*, and *AtAHA2* were individually cloned as prey in the *pDEST22* vector, and different combinations of bait and prey vector were cotransformed into MVA201 yeast cells. The *GCN4* AAAD1 and AAAD2 domains were expressed independently in *pDEST22* vector. Krev1 RalGDS and Krev1 RalGDS-m1 were used as positive and negative controls, respectively, and grown on double (-Leu, -Trp), triple (-Leu, -Trp, -His + 20 mM 3-aminotriazole [3AT]), or quadruple (-Leu, -Trp, -His, -Ura + 20 mM 3AT) dropout medium.

(B) BiFC assay with split EYFP confirms the interaction of AtGCN4 with AtRIN4 or At14-3-3 in planta. The *pSITE-nEYFP-GCN4* construct was coexpressed with *pSITE-RIN4-cEYFP* or *pSITE-14-3-3-cEYFP* in *N. benthamiana* using Agrobacterium-mediated transient expression. Similarly, *pSITE-nEYFP-AAAD1* and *pSITE-nEYFP-AAAD2* were coexpressed with *pSITE-RIN4-cEYFP* or *pSITE-14-3-3-cEYFP in N. benthamiana*. After 2 d, images were taken using a confocal microscope. DIC, differential interference contrast image. Bars = 50 μm.

containing either the AAAD1 or AAAD2 domain was not able to interact with RIN4, whereas it interacted weakly with 14-3-3 (Figure 7A). Yeast expressing either GCN4 or truncated GCN4 containing mainly either the AAAD1 or AAAD2 domain or RIN4 or 14-3-3 protein did not grow in triple dropout medium when co-transformed with empty vector (Supplemental Figure 9A). Krev1 (Rap1A; a member of the Ras family of GTP binding proteins) RalGDS (Ral guanine nucleotide dissociator stimulator protein; Herrmann et al., 1996; Serebriiskii et al., 1999) and Krev1 RalGDS-m1 (a mutant version of RalGDS) were used as positive and negative controls, respectively. Further, a bimolecular fluorescence complementation (BiFC) assay in *N. benthamiana* by transient coexpression of *AtGCN4* fused to the N-terminal half of the enhanced yellow fluorescent protein (*EYFP*) and *AtRIN4* or *At14-3-3* fused to the C-terminal half of *EYFP* reconstituted the expression of *YFP* in the PM (Figure 7B). Consistent with the Y2H results, the truncated GCN4 containing mainly either the AAAD1 or AAAD2 domain did not interact with RIN4 by BiFC (Figure 7B). Consistent with the Y2H results, the AAAD1 domain of GCN4 interacted with 14-3-3. Interestingly, the AAAD2 domain of GCN4 that interacted weakly with 14-3-3 in the Y2H assay was not able to interact with 14-3-3 in the BiFC assay. None of these constructs when infiltrated alone was able to produce any fluorescence (Supplemental Figure 9B). To further biochemically confirm this in vivo interaction, *AtGCN4-GFP* was expressed in *N. benthamiana* by agroinfiltration and *AtRIN4-GST* or *At14-3-3-GST* was expressed in *Escherichia coli*. Protein extracts from *N. benthamiana* and purified recombinant protein from *E. coli* were subjected to coimmunoprecipitation (co-IP) assays. AtGCN4-GFP fusion protein was able to coimmunoprecipitate both AtRIN4-GST and At14-3-3-GST either individually or together (Figure 8A). Overall, these data suggest that GCN4 interacts with RIN4 and 14-3-3 proteins in vitro and in planta.

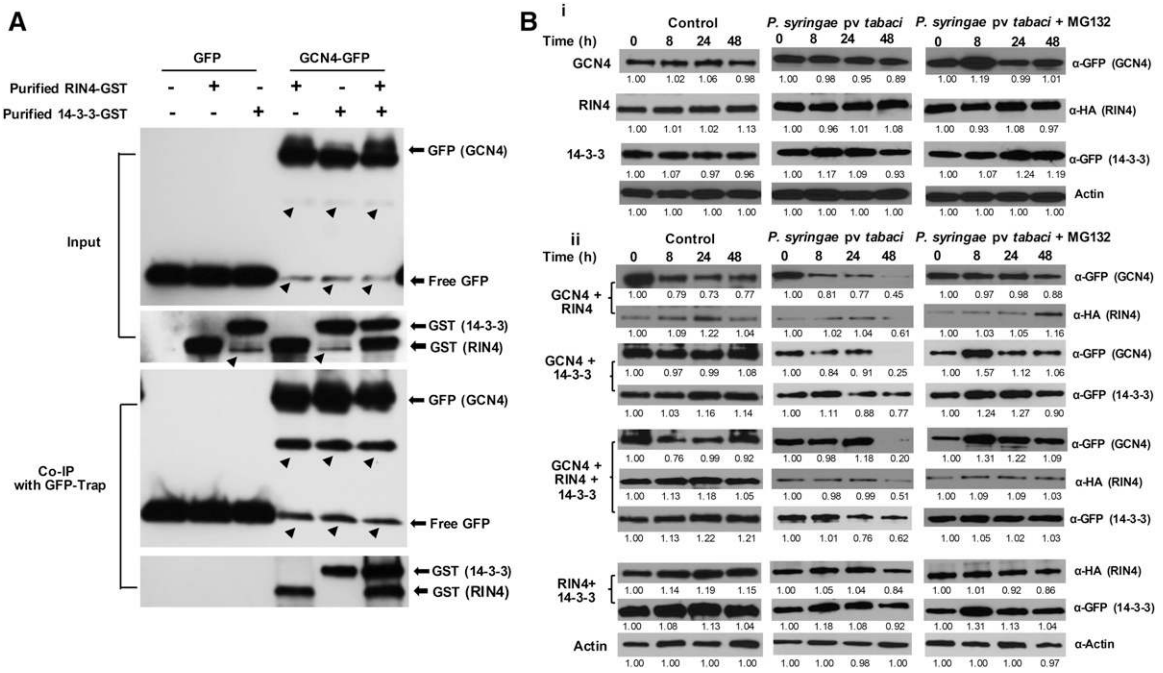

Figure 8. GCN4 Degrades RIN4 and 14-3-3 via a Proteasome-Mediated Pathway.

(A) Co-IP assay showing the biochemical interaction of AtGCN4 with AtRIN4 and At14-3-3 in semi-in vivo conditions. The *AtGCN4-GFP* construct was expressed in *N. benthamiana* using Agrobacterium-mediated transient expression. *AtRIN4-GST* and *At14-3-3-GST* cloned in *pDEST17* were expressed in *E. coli*, and proteins were purified and confirmed by immunoblotting with GFP or GST antiserum (black arrowheads indicate nonspecific or degraded proteins). An equal amount of AtGCN4-GFP was used in the co-IP assays. Input and bound forms of RIN4 and 14-3-3 were detected using GST antibody. Co-IP assays were performed at 4°C, and protein gel blot analysis was performed using anti-GST antibody.

(B) (i) When individually expressed in *N. benthamiana*, GCN4, RIN4, and 14-3-3 proteins did not degrade upon host pathogen (*P. syringae* pv *tabaci*) treatment. (ii) GCN4 showed degradation upon pathogen inoculation when coexpressed with either RIN4 or 14-3-3. RIN4 and 14-3-3 were also degraded upon coexpression with GCN4 at 48 hpi with the host pathogen. Leaves treated with the proteasome inhibitor MG132 (2 μM) during pathogen infection exhibited reduced degradation of RIN4, 14-3-3, and GCN4. Proteins were analyzed by immunoblotting using HA tag and GFP tag antisera. Numbers below indicate the ratio of band intensity compared with 0 hpi. Actin was used as a loading control.

GCN4 Reduces the Activity of the PM H$^+$-ATPase Complex Probably by Degrading RIN4 and 14-3-3 Proteins via the Proteasome Pathway

To elucidate the function of GCN4's interaction with RIN4 and 14-3-3, AtGCN4-GFP-, HA-AtRIN4-, and At14-3-3-GFP-tagged proteins were transiently expressed either independently or in combination in *N. benthamiana* by *Agrobacterium tumefaciens*-mediated transient transformation. After 2 d, the host pathogen *P. syringae* pv *tabaci* was sprayed on the leaves in which the recombinant proteins were expressed, and tissue was harvested at 0, 8, 24, and 48 hpi and analyzed for the expression of proteins. All the proteins were stably expressed when they were expressed alone, and the protein amounts were not significantly reduced upon pathogen infection (Figure 8B). Interestingly, upon coexpression of *GCN4* and *RIN4*, the level of GCN4 protein was slightly reduced at 8 hpi, and the reduction was more drastic at 48 hpi. Upon coexpression of *GCN4* and *14-3-3*, the level of GCN4 protein was reduced only at 48 hpi. GCN4 protein levels were not reduced following the addition of the proteasome inhibitor MG132 (Figure 8B). The levels of RIN4 and 14-3-3 proteins were also reduced when coexpressed with *GCN4* at 48 hpi with pathogen. Again, this reduction was not observed in the presence of MG132 (Figure 8B). Upon coexpression of *RIN4* and *14-3-3*, their protein levels were not significantly reduced in the absence of GCN4 even after pathogen infection. These data suggest that RIN4 and 14-3-3 proteins are probably degraded via the proteasome pathway in the presence of GCN4 in response to pathogen inoculation.

DISCUSSION

Many bacterial pathogens enter plant tissue through natural openings such as stomata and hydathodes and colonize the apoplastic space of host plants (Wang et al., 2012). Plants have an active defense response to close stomata upon perceiving pathogens (Melotto et al., 2006). We identified a AAA$^+$-ATPase gene (*GCN4*) that plays a novel role in stomata-mediated plant defense. AAA$^+$-ATPase proteins have been shown to play a role in plant defense responses such as HR in tobacco (*Nicotiana tabacum*; Sugimoto et al., 2004). Proteasome REGULATORY PARTICLE BASE SUBUNIT6 (RPT6), a component of the 26S proteasome belonging to the AAA$^+$-ATPase class, has been shown to be targeted by bacterial effectors such as HopZ, XopJ, and YopZ to cause disease (Üstün et al., 2015). Our data showed

that overexpression of *AtGCN4* in Arabidopsis reduced bacterial accumulation in the apoplast due to closed stomata that could not be reopened by virulent bacteria. *P. syringae* pv *tomato* strain DC3000 produces a phytotoxin, COR, that has been shown to reopen stomata within 3 hpi in Arabidopsis (Melotto et al., 2006). COR acts as a structural mimic of JA conjugates and by binding to the F-box-containing JA receptor COR INSENSITIVE1 (COI1) degrades the JASMONATE ZIM domain (JAZ) proteins to activate MYC2 target transcripts. However, the precise role of COR in stomatal opening is not known (Underwood et al., 2007). Recently, it was shown that AHA1 promotes COI1 and JAZ protein interaction and enhances JA signaling that is required for optimum stomatal infection (Zhou et al., 2015). *AtGCN4*-overexpressing and Col-0 plants, but not *AtGCN4* RNAi lines, were able to close stomata upon treatment with ABA (Figures 3A and 3B). However, in response to ABA followed by COR or fusicoccin treatment, the stomata remained open in wild-type plants but closed in the overexpression lines.

AAA$^+$-ATPases in all organisms are involved in protein degradation and act as key components of the 26S proteasomal complex (Hanson and Whiteheart, 2005; Bar-Nun and Glickman, 2012). For example, the well-studied *N*-ethylmaleimide-sensitive factor (NSF) is a homohexameric AAA$^+$-ATPase involved in the transfer of membrane vesicles from one membrane compartment to another through an ATP hydrolysis mechanism. Soluble NSF attachment protein receptors (SNAREs) are involved in diverse mechanisms, including protein trafficking, cell homeostasis, morphogenesis, and pathogen defense (Wick et al., 2003; Zhang et al., 2015). Several SNARE proteins are induced upon pathogen stress. For example, *AtSNAP33* was induced in response to pathogens such as *Plectosporium tabacinum*, virulent and avirulent forms of *Peronospora parasitica*, and *P. syringae* pv *tomato* (Wick et al., 2003). The interaction of the K$^+$ channel proteins KAT1 (K$^+$ transporter) and KC1 (K$^+$ channel) with Arabidopsis R-SNARE VAMP721 (vesicle-associated membrane proteins) showed the regulation of K$^+$ ion gates at the PM (Zhang et al., 2015). The *AtGCN4*-overexpressing Arabidopsis plants showed a closed-stomata phenotype only after biotic or abiotic stimuli (Figures 6A and 6B). Based on our results and the reported function of AAA$^+$-ATPases, we speculated that constitutive overexpression of *AtGCN4* may reduce the activity of the H$^+$ proton pump complex to keep stomata closed during pathogen infection. To validate this hypothesis, we showed that AtGCN4 interacted directly with RIN4 and 14-3-3 proteins that are part of the PM H$^+$-ATPase complex (Liu et al., 2009; Figures 7A, 7B, and 8A). Degradation of RIN4 and 14-3-3 proteins through a proteasome-mediated pathway was observed in the presence of *GCN4* overexpression and pathogen infection (Figure 8B). It is intriguing that degradation of RIN4 and 14-3-3 was observed only after pathogen inoculation. We speculate that in wild-type Arabidopsis, the endogenous levels of GCN4 are not sufficient to trigger the degradation of the RIN4/14-3-3 complex and, therefore, the stomata can be reopened by bacteria. We have shown that *GCN4* is induced upon pathogen inoculation (Figure 2C), and this may change the stoichiometry of the GCN4-RIN4-14-3-3 protein complex. We propose that the stoichiometry of the protein complex is important for triggering protein degradation.

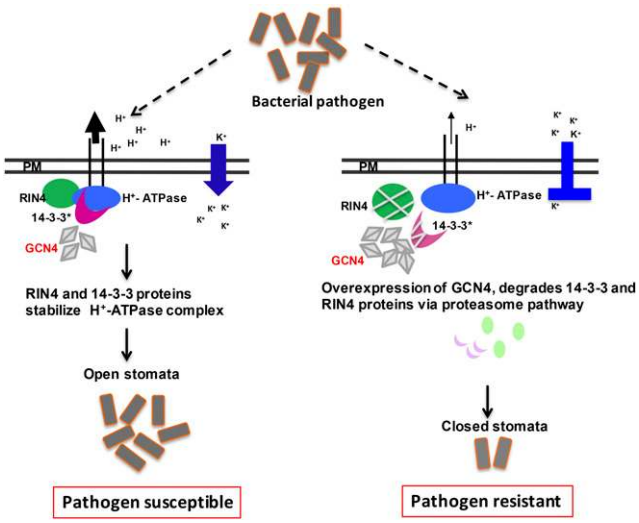

Figure 9. A Model for GCN4-Mediated Regulation of Stomatal Aperture and Plant Immunity.

Pathogens target RIN4 and 14-3-3 to phosphorylate AHA1 and AHA2 and stabilize the H$^+$-ATPase complex to activate the H$^+$-ATPase proton pump to open stomata (left panel). Constitutive overexpression of *GCN4* degrades RIN4 and 14-3-3 proteins through a proteasome-mediated mechanism and inhibits H$^+$-ATPase activity to reduce proton pump activity, thereby closing stomata and restricting pathogen entry (right panel). Green, RIN4 protein; pink, 14-3-3 protein; gray, GCN4 protein. Multiple gray diamonds indicate overexpression of GCN4.

GCN4-overexpressing Arabidopsis plants were resistant to bacterial pathogens (Figures 3E and 3F). By contrast, *GCN4*-silenced plants cannot close stomata due to biotic stimuli and hence are more susceptible to host and nonhost pathogens. As one of the plausible mechanisms, we speculate that the overexpression of *GCN4* enhances the removal (degradation) of RIN4 and 14-3-3 proteins from the AHA1 and AHA2 complexes, resulting in reduced H$^+$-ATPase activity and, hence, stomata remain closed even upon virulent pathogen infection (Figure 9). Perhaps induction of *GCN4* expression upon pathogen infection (Supplemental Figures 2C and 6B) is part of the plant defense response to close stomata. Considering the broader function of AAA-ATPase proteins, *GCN4* may also have other functions in plant processes that need to be explored. Further, we speculate that adapted or virulent pathogens can interfere with GCN4-mediated stomatal closure or can regulate stomatal opening through a different pathway in wild-type plants. It is known that some *P. syringae* strains secrete effector proteins that suppress stomatal immunity (Lozano-Durán et al., 2014). We speculate that overexpression of *GCN4* in plants can suppress effector-mediated reopening of stomata. Apart from playing a role in stomata-mediated plant defense, GCN4 also seems to be involved in other plant innate immune responses. For example, *GCN4*-silenced plants were susceptible to nonhost pathogens even when inoculated by syringe infiltration, which bypasses stomatal entry of the pathogen (Figures 1 and 3). In addition, *NbGCN4*-silenced *N. benthamiana* plants showed a delay in producing nonhost HR when compared with a nonsilenced control (Figure 1D). Future studies should examine the role of GCN4 in

apoplastic defense responses. Nevertheless, our discovery of a previously unknown function of GCN4 in regulating the RIN4- and 14-3-3-containing PM H^+-ATPase complex provides significant insights that can be applied in crop improvement programs aiming to develop pathogen-resistant and/or drought-tolerant crops.

METHODS

Gene Constructs, Bacterial Strains, and Plant Materials

Agrobacterium tumefaciens strain GV3101 containing TRV2:*4D7-2* (NbME04D07-2; http://vigs.noble.org) was grown at 28°C in Luria-Bertani medium supplemented with rifampicin (10 μg/mL) and kanamycin (50 μg/mL). VIGS was performed by mixing a 1:1 ratio of Agrobacterium strains containing TRV1 and TRV2 as described (Senthil-Kumar and Mysore, 2014). *Pseudomonas syringae* strains were grown in King's B medium at 30°C supplemented with rifampicin (10 μg/mL), kanamycin (50 μg/mL), or streptomycin (50 μg/mL) when needed. The *Arabidopsis thaliana GCN4* full-length CDS was expressed in pMDC32 vector (Curtis and Grossniklaus, 2003) with *2X35S* promoter. Several putative *gcn4* T-DNA insertion mutants (SAIL_589_H02.v2, SALK_080928, SALK_040028, SALK_040028.36.55.x, SALK_040028.56.00.x, SALK_040124.37.50.x, SALK_109597.47.30.x, SALK_017235.55.25.x.) are listed in the SALK database. We obtained these mutants and, after molecular characterization, realized that none of them are complete knockouts. Therefore, we decided to generate *GCN4* RNAi lines. To generate *AtGCN4* RNAi lines, pH7GWIW G2 (II) vector (https://gateway.psb.ugent.be/search/index/silencing/any) with two different ~250-bp fragments of the AtGCN4 CDS from 395 to 620 bp (RNAi A4) or 1211 to 1460 bp (RNAi B1) was used. For co-IP studies, *GCN4* was expressed in Gateway destination vector pMDC83 with GFP tag on the C terminus by Gateway cloning (http://www.botinst.uzh.ch/en/research/development/grossnik/vectors/MarkdGatewayVectors.html). Both *14-3-3* and *RIN4* were expressed in the pDEST15 vector with the GST tag. For the immunoblot or protein degradation assay, *GCN4-GFP* was expressed in pMDC83, and 14-3-3-HA and RIN4-HA were expressed in the pEARLEYGATE 201 vector. To express *GCN4-GFP* under the control of its native promoter, *GCN4* was cloned into the pMDC107 vector. Floral dip inoculation (Clough and Bent, 1998) was used to develop transgenic lines that were screened on hygromycin (25 μg/mL) and basta (25 μM/mL).

Phylogenetic Analysis

Amino acid sequences for the candidate *GCN4* genes from different species were identified from the BLAST homology analysis. Sequence alignments were made using the geneious tool (http://www.geneious.com) and further refined. Bootstrapping was performed with stepwise addition of 1000 replicates. A phylogenetic tree was computed, annotated, and depicted using the geneious tool. The phylogenetic tree is also reconfirmed by the Molecular Evolutionary Genetic Analysis (MEGA 6.0) alignment tool (http://www.megasoftware.net).

Disease Development and HR Assay in *Nicotiana benthamiana*

Four-week-old *N. benthamiana* seedlings were inoculated with an Agrobacterium strain containing TRV:*NbGCN4*. Three weeks after TRV inoculation, the silenced and nonsilenced plants were vacuum infiltrated with host or nonhost pathogens. To study the role of *NbGCN4* in HR to nonhost pathogens, the silenced and control plants were infiltrated with nonhost pathogens. To determine the bacterial titer, leaf discs at 0, 1, 2, 3, 5, and 7 dpi, from four biological replicates representing four individual plants, were collected using a 1-cm^2 core borer. Leaf samples were ground, subjected to serial dilution, plated on King's B agar medium supplemented with appropriate antibiotics, and incubated at 28°C for 2 d for bacterial colony counting. For visualization of bacterial multiplication using *GFPuv*-expressing strains, plants were syringe infiltrated as described (Wang et al., 2007).

In Planta Bacterial Number and Disease Development in Arabidopsis

For flood inoculation, 4-week-old plants grown on Murashige and Skoog plates were incubated for 1 min with 40 mL of bacterial suspension as described (Ishiga et al., 2011). Symptoms were observed after 5 d. To examine bacterial growth, the entire rosette was harvested, ground, and serially diluted as described (Ishiga et al., 2011). For syringe inoculation, 6-week-old plants were infiltrated on the abaxial side of the leaves with the pathogen. Leaf samples from three biological replicates from three individual plants were collected, and the bacteria were quantified as described above for *N. benthamiana*.

Gene Expression Analyses

To test the downregulation of *GCN4* transcripts in *N. benthamiana* silenced plants, tissue was collected 3 weeks after TRV inoculation. To determine the expression of *GCN4* in the Arabidopsis wild type (Col-0), plants were treated with the host pathogen *P. syringae* pv *maculicola* (1×10^4 cfu/mL) and the nonhost pathogen *P. syringae* pv *tabaci* (1×10^4 cfu/mL) by flood inoculation, and leaf tissue was collected at 12 and 24 hpi. Total RNA was extracted according to the manufacturer's instructions using a Qiagen Total RNA Extraction Kit. The cDNA was synthesized by oligo(dT) primers using moloney murine leukemia virus reverse transcriptase (Thermo Fisher Scientific) according to the manufacturer's instructions. RT-qPCR was performed with the Sigma-Aldrich KicQStart SYBR Green Kit. The conditions for the PCR were as follows: 95°C for 2 min, 25 cycles of denaturation at 94°C for 45 s, annealing for 30 s at 58°C, and polymerization for 45 s at 72°C, followed by plate reading at 72°C for 5 min, estimation of melting curve from 50 to 95°C, and incubation at 72°C for 4 min. The Arabidopsis *Actin* gene was used as a reference to normalize RT-qPCR, and expression was quantified as described (Ruijter et al., 2009). The primers used in the study are given in Supplemental Table 1.

Localization of GCN4

For the subcellular localization assay, native promoter-driven *AtGCN4* was fused to the N-terminal part of *GFP* and cloned into the binary vector *pMDC107*. Stable Arabidopsis transgenic lines were developed by floral dip transformation, and GFP fluorescence was captured using a Perkin-Elmer ultraview spinning disk confocal microscope. For extraction of the PM fraction and cytosolic fraction proteins, 13-d-old stable AtGCN4-GFP Arabidopsis plants were harvested and then homogenized in homogenization buffer (50 mM MOPS, pH 7.0, 5 mM EDTA, 0.33 M sucrose, 1.5 mM ascorbate, 0.2% [w/v] insoluble polyvinylpolypyrrolidone, 2 mM DTT, 1 mM PMSF, 1 μg/mL leupeptin, and 1 μg/mL pepstatin A) on ice. The homogenate was filtered through a 240-μm nylon net and centrifuged at 700*g* for 10 min at 4°C. The PM Protein Extraction Kit (ab65400; Abcam) was used to extract PM and cytosol proteins. GFP antibody (lot number 120-002-105, catalog number 130-091-833; Miltenyl Biotec) was used to detect GCN4, and H^+-ATPase antibody (lot number 1510, catalog number ABIN1720784; Abcam) was used as a PM marker protein.

To test the tissue-specific expression of *GCN4*, the *pGCN4:GCN4-GUS* construct was cloned into the binary vector pMDC162. The stable transgenic lines expressing AtGCN4-GUS were developed by floral dip transformation (Mara et al., 2010). After selecting the stable lines on hygromycin, the whole plants were stained with X-gluc substrate (Jefferson et al., 1987). To see the expression of *GCN4* in guard cells, the leaf samples were analyzed under a microscope.

Drought Stress Imposition and Measurement of Water Loss

The moisture stress was imposed on Col-0, RNAi, and overexpression lines by gradual reduction of water by bringing the field capacity from 100 to 40% in 9 d (Babitha et al., 2013). The pots were filled with a known quantity of soil and completely saturated with water to arrive at the amount of water required to maintain 100% field capacity. Gradual moisture stress was imposed by weighing the pots, and the loss of water in the pots was replenished with the required amount of water to arrive at the desired field capacity of the soil. At the end of the stress period, the pots reached 35% field capacity. The duration of stress imposition was for a period of 9 d. The plants were allowed to recover by rewatering for 10 d. To measure relative water loss, the detached leaves from 4-week-old plants were air dried at room temperature, the weight of leaves was determined every 1 h, and relative water loss percentage was calculated over the initial leaf weight.

Measurement of Stomatal Aperture

Fresh leaves from 3-week-old plants at similar developmental stages were harvested. The epidermal peels from leaves were then incubated in stomata opening buffer (5 mM KCl, 50 mM $CaCl_2$, and 10 mM MES-Tris, pH 6.1) or 0.5 ng/μL COR (purchased from C. Bender, Oklahoma State University), or 1 ng/μL fusicoccin (Sigma-Aldrich) or 10 μM ABA (Sigma-Aldrich), or pathogens or various combinations at room temperature under high light for 3 h. Photographs were taken using a Nikon Optishot-2 camera at 40×, and stomatal apertures were measured using ImageJ software (Chitrakar and Melotto, 2010).

PM H^+-ATPase Activity Assay

Various Arabidopsis lines were grown for 5 weeks in soil at pH 7.5. *RIN4*-expressing lines were sprayed with 20 mM dexamethasone in 0.025% Silwet, while the remaining lines were sprayed with water and 0.025% Silwet. Leaf tissue was harvested after 48 h. One set of plants was used as a control without pathogen treatment and another set of plants was sprayed with *P. syringae* pv *tomato* (DC3000), and tissue was harvested after 4 h. For all experiments, PM was immediately purified after harvesting leaf tissue (Liu et al., 2009). H^+-pump activity was detected by a decrease of acridine orange absorbance at 495 nm as described (Liu et al., 2009). The assay buffer contained 20 mM MES-KOH, pH 7.0, 140 mM KCl, 3 mM ATP-Na_2, 30 mM acridine orange, 0.05% Brij 58, and 50 mg of PM protein in a total volume of 1 mL. Membranes were preincubated at 25°C for 5 min in assay buffer. The assay was initiated by the addition of 3 mM $MgSO_4$. Each experiment was repeated two times with independent PM isolations.

Isolation of Guard Cells and RNA Extraction

Arabidopsis Col-0 plants were grown under 8-h-light (300 μmol m^{-1} s^{-1} with LED bulbs)/16-h-dark conditions for 5 weeks. Plants were sprayed with either 4.0×10^7 cfu/mL *P. syringae* pv *tabaci* or *P. syringae* pv *tomato* (DC3000) in water containing 0.025% Silwet L-77 or with water containing 0.025% Silwet L-77 as mock. Guard cell enrichment was done as described with slight modification (Misra et al., 2015). Ten grams of leaves with main veins removed was harvested and blended four times for 20 s each in 100 mL of cold sterile distilled water with the transcription inhibitors cordycepin (0.01%) and actinomycin D (0.0033%) using a Waring Laboratory Blender (http://www.waringlab.com/). Transcription inhibitors were used to inhibit the potential induction of transcript during guard cell enrichment (Obulareddy et al., 2013). The blended mixture was filtered through a 100-μm nylon mesh (sefar.com), and remnant was washed with cold distilled water until the flow-through was clear of mesophyll cells, debris, and plastids. These epidermal peels were digested with a mixture of 0.7% cellulysin and 0.025% macerozyme R10 with 0.1% polyvinylpyrrolidone 40 and 0.25% BSA for 1 h in darkness with shaking at 140 rpm. The digest was washed on a 100-μm nylon mesh using 750 mL of cold basic solution (560 mM sorbitol, 5 mM MES, 0.5 mM $CaCl_2$, 0.5 mM $MgCl_2$, and 10 μM KH_2PO_4, pH 5.5) to remove broken epidermal cells. Guard cell enrichment was verified by observing a small portion of tissue under a Nikon Optiphot-2 microscope (Nikon Instruments). RNA was isolated from guard cell-enriched tissue using TRIzol reagent (Life Technologies), and cDNA synthesis and RT-qPCR analysis were performed as described previously (Pant et al., 2015). In brief, RNA was treated with DNase I using the TURBO DNA-free Kit (Thermo Fisher Scientific) according to the manufacturer's instructions, and cDNA was synthesized from 1 μg of RNA using SuperScript III Reverse Transcriptase (Thermo Fisher Scientific) according to the manufacturer's instructions. The expression profiling of genes was performed using a 7900HT Real-Time PCR System (Thermo Fisher Scientific). Enrichment of guard cells was also verified at the molecular level by checking the expression of *At5g46240* (*KAT1*) and *At1g62400* (*HT1*) transcripts known to be induced in guard cells (Bates et al., 2012). The experiment was repeated using independently grown plant material.

Recombinant Protein Expression and ATPase Activity of GCN4

To determine if purified GCN4 protein has ATPase activity, the GCN4-His-tagged protein was overexpressed in *Escherichia coli* BL21 expression cells using *pDEST17* vector and induced with IPTG. The protein was purified using Ni-NTA agarose (Qiagen). Protein was confirmed by His tag-specific antiserum (catalog number H1029, batch number 033M4785; Sigma-Aldrich) by protein blotting. To determine ATPase activity, an EnzChek Phosphate Assay Kit was used (Thermo Fisher Scientific). Three milligrams of purified recombinant GCN4 protein was added to the assay medium and preincubated at 25°C for 10 min before the addition of $MgSO_4$. The Bradford assay was used to calculate total protein content (Bradford, 1976).

Yeast Two-Hybrid Assays

Yeast two-hybrid assays were performed following the manufacturer's protocol using the ProQuest Two-Hybrid System (Thermo Fisher Scientific). AtGCN4 was fused to the GAL4 DNA binding domain in *pDEST32* as the bait construct. AtRIN4, At14-3-3, AtAHA1 (At2g18960), and AtAHA2 (At4g30190.2) proteins were used as prey proteins and fused to the GAL4 activation domain in *pDEST22*. The AAAD1 and AAAD2 domains of GCN4 were expressed separately in *pDEST32* vector. Bait and prey constructs were cotransformed into yeast MaV203 competent cells. Positive clones were identified by their ability to grow on synthetic defined medium minus Leu/Trp/His (triple dropout medium) or Leu/Trp/His/Ura (quadruple dropout medium) containing 20 mM 3-aminotriazole. Liquid medium contained X-Gal to detect interaction by the development of blue color.

BiFC Assay

AtGCN4 was fused to the N-terminal *EYFP* in the *pSITE-nEYFP* vector. *AtRIN4* and *At14-3-3* were fused with the C-terminal part of *EYFP* in *pSITE-cEYFP* (Kudla and Bock, 2016). The AAAD1 and AAAD2 domains of *GCN4* were expressed separately in the N-terminal *pSITE-nEYFP* vector. These vectors were transiently expressed in *N. benthamiana*. Leaves were collected 3 d after infiltration. Fluorescence was detected using either a Leica TCS SP2 or a Bio-Rad MRC 1024 ES confocal laser-scanning microscope.

Co-IP Assay

For immunoprecipitation and co-IP assays, *N. benthamiana* leaves were harvested 2 d after infiltration with an Agrobacterium strain containing the *Pro35S:GCN4* construct within the T-DNA and were homogenized in

protein extraction buffer (50 mM Tris-HCl, pH 7.5, 75 mM NaCl, 0.2% Triton X-100, 5 mM EDTA, 5 mM EGTA, 1 mM DTT, 100 μM MG132, 10 mM NaF, 2 mM Na_2VO_4, and 1% protease inhibitor cocktail [P9599; Sigma-Aldrich]). The interacting proteins RIN4 and 14-3-3 were individually expressed with C-terminal GST tag in *pDEST15*-expressing rosette cells. The proteins were purified with GST resin and confirmed by GST-specific antisera (lot number GR 9, 3884-10, catalog number ab58626; Abcam). The protein content was quantified using a Pierce 660-nm protein assay reagent (Thermo Fisher Scientific). After protein extraction, 5 μg of purified RIN4/14-3-3 from *E. coli* was added to 100 μg of total protein and incubated overnight at 4°C. The mixture was incubated for 2 h at 4°C with GFP Trap-A (Chromotek). The precipitated samples were washed, released by 2× SDS protein loading buffer, resolved by SDS-PAGE, and then transferred to nitrocellulose membranes. These membranes were incubated in blocking buffer (1× Tris-buffered saline buffer including 0.1% Tween 20 and 5% dried nonfat milk) for 1 h at room temperature, then with horseradish peroxidase-conjugated anti-GFP (Miltenyl Biotec) and anti-GST (Abcam) antibodies overnight at 4°C. An enhanced chemiluminescence system (GE Healthcare) was used for detection (Golemis, 2002).

Protein Degradation and Gel Blot Analyses

GCN4-GFP, HA-RIN4, and 14-3-3-GFP recombinant proteins were transiently expressed either individually or coexpressed in various combinations in *N. benthamiana* leaves using Agrobacterium. The bacterial infiltrations were performed with the same Agrobacterium concentration (0.6 OD_{600}) for all the constructs. Total protein was quantified using the Bradford method, and equal known concentrations were taken for the protein degradation assay. After 48 hpi with Agrobacterium, the host pathogen *P. syringae* pv *tabaci* was infiltrated at the same spot where Agrobacterium was infiltrated, and tissue was frozen after 0, 8, 12, 24, and 48 hpi. Total protein was extracted from leaf samples with extraction buffer (50 mM Tris-MES, pH 7.5, 80 mM NaCl, 10 mM $MgCl_2$, 10% glycerol, 0.2% Nonidet P-40, 1 mM EDTA, 1 mM PMSF, and protease inhibitor cocktail [Sigma-Aldrich]). Samples were incubated at room temperature. MG132 (1.6 μM; Sigma-Aldrich) was added to part of the samples to inhibit the proteasome-mediated protein degradation. Later, proteins were blotted on PVDF membrane, and GFP antiserum (Miltenyl Biotec) or HA antiserum (Sigma-Aldrich) was used to detect the GCN4, RIN4, and 14-3-3 protein levels. Actin antiserum (catalog number A0480, lot number 054M4805V; Sigma-Aldrich) was used to detect endogenous Actin protein that served as a loading control. The primary horseradish peroxidase-conjugated GFP, HA, and Actin antisera were diluted to 1:10,000 followed by secondary goat anti-rabbit antibody (lot number GR 1, 46572-6, catalog number ab9110; Abcam) conjugated to horseradish peroxidase and visualized using enhanced chemiluminescence solution (GE Healthcare Bio-Sciences), and protein gel blots were imaged.

Accession Numbers

Sequence data from this article can be found in the GenBank data library under accession numbers At3g54540 (AtGCN4), NbME04D07-2 (NbGCN4), At3g25070 (AtRIN4), At1g34760 (At14-3-3), At2g18960 (AtAHA1), and At4g30190.2 (AtAHA2).

Supplemental Data

Supplemental Figure 1. Silencing of *4D7-2* in *N. benthamiana* Compromises Nonhost Disease Resistance.

Supplemental Figure 2. *AtGCN4* Overexpression and RNAi Lines.

Supplemental Figure 3. Arabidopsis Plants Overexpressing *AtGCN4* Are Resistant to Host Pathogen *P. syringae* pv *maculicola* upon Flood Inoculation.

Supplemental Figure 4. AtGCN4 Localizes to PM and Guard Cells.

Supplemental Figure 5. Scanning Electron Micrographs of the Adaxial Leaf Surface of Col-0, *AtGCN4*-RNAiA4, *AtGCN4*-RNAiB1, *AtGCN4*-OE6 and *AtGCN4*-OE16 at Magnification of 100 μm and 20 μm.

Supplemental Figure 6. Expression of Recombinant AtGCN4 Protein in *Escherichia coli* to Determine ATPase Activity.

Supplemental Figure 7. Stomatal Closure on *AtGCN4* RNAi Lines Is Insensitive to Fusicoccin, Coronatine, and Nonhost Pathogen *P. syringae* pv *tabaci*.

Supplemental Figure 8. Open Stomata Phenotype in *Nb4D7-2 (NbGCN4)* Silenced *N. benthamiana* Plants upon Nonhost Pathogen Infection.

Supplemental Figure 9. A Negative Control for Y2H Assay and Bimolecular Fluorescence Complementation Assay with Split Enhanced Yellow Fluorescent Protein.

Supplemental Table 1. List of Primers Used in the Study.

Supplemental Data Set 1. GCN4 Sequence and Its Alignment with Its Orthologs.

ACKNOWLEDGMENTS

We thank Gitta Coaker (University of California, Davis) for providing *RIN4* overexpression and *rin4* mutant seeds and Janie Gallaway for assistance with plant care. This work was supported by the Noble Research Institute. The Leica confocal system used in this study was purchased using a National Science Foundation grant (Grant DBI 0400580). V.S.R. acknowledges a Fulbright-Nehru postdoctoral fellowship from USIEF, India.

AUTHOR CONTRIBUTIONS

A.K. and K.S.M. conceived the project and designed the experiments. A.K. identified and cloned *GCN4*, developed the transgenic lines, performed the disease assays, and conducted the Y2H and BiFC experiments. V.S.R. and S.O. performed the drought tolerance, GCN4 ATPase activity, PM H^+-ATPase activity, protein expression, co-IP, and protein degradation assays. C.M.R. helped with the protein purification and edited the article. H.-K.L. assisted in the genotyping of transgenic lines. S.L. performed stomatal aperture measurements. M.S.-K. performed VIGS in *N. benthamiana*. B.P. isolated the guard cells and performed stomatal aperture measurements. A.K., V.S.R., and K.S.M. wrote the article.

Received January 26, 2017; revised July 13, 2017; accepted August 28, 2017; published August 30, 2017.

REFERENCES

Arnaud, D., and Hwang, I. (2015). A sophisticated network of signaling pathways regulates stomatal defenses to bacterial pathogens. Mol. Plant **8:** 566–581.

Babitha, K.C., Ramu, S.V., Pruthvi, V., Mahesh, P., Nataraja, K.N., and Udayakumar, M. (2013). Co-expression of AtbHLH17 and AtWRKY28 confers resistance to abiotic stress in *Arabidopsis*. Transgenic Res. **22:** 327–341.

Bar-Nun, S., and Glickman, M.H. (2012). Proteasomal AAA-ATPases: structure and function. Biochim. Biophys. Acta **1823:** 67–82.

Bates, G.W., Rosenthal, D.M., Sun, J., Chattopadhyay, M., Peffer, E., Yang, J., Ort, D.R., and Jones, A.M. (2012). A comparative study of the *Arabidopsis thaliana* guard-cell transcriptome and its modulation by sucrose. PLoS One **7:** e49641.

Baunsgaard, L., Fuglsang, A.T., Jahn, T., Korthout, H.A., de Boer, A.H., and Palmgren, M.G. (1998). The 14-3-3 proteins associate with the plant plasma membrane H^+-ATPase to generate a fusicoccin binding complex and a fusicoccin responsive system. Plant J. **13:** 661–671.

Bradford, M.M. (1976). A rapid and sensitive method for the quantitation of microgram quantities of protein utilizing the principle of protein-dye binding. Anal. Biochem. **72:** 248–254.

Chitrakar, R., and Melotto, M. (2010). Assessing stomatal response to live bacterial cells using whole leaf imaging. J. Vis. Exp. **44:** e2185.

Clough, S.J., and Bent, A.F. (1998). Floral dip: a simplified method for *Agrobacterium*-mediated transformation of *Arabidopsis thaliana*. Plant J. **16:** 735–743.

Cui, H., Wang, Y., Xue, L., Chu, J., Yan, C., Fu, J., Chen, M., Innes, R.W., and Zhou, J.M. (2010). *Pseudomonas syringae* effector protein AvrB perturbs *Arabidopsis* hormone signaling by activating MAP kinase 4. Cell Host Microbe **7:** 164–175.

Curtis, M.D., and Grossniklaus, U. (2003). A gateway cloning vector set for high-throughput functional analysis of genes in planta. Plant Physiol. **133:** 462–469.

Del Carmen Martínez-Ballesta, M., Moreno, D.A., and Carvajal, M. (2013). The physiological importance of glucosinolates on plant response to abiotic stress in Brassica. Int. J. Mol. Sci. **14:** 11607–11625.

Fan, J., Crooks, C., Creissen, G., Hill, L., Fairhurst, S., Doerner, P., and Lamb, C. (2011). *Pseudomonas sax* genes overcome aliphatic isothiocyanate-mediated non-host resistance in Arabidopsis. Science **331:** 1185–1188.

Fujita, Y., Fujita, M., Satoh, R., Maruyama, K., Parvez, M.M., Seki, M., Hiratsu, K., Ohme-Takagi, M., Shinozaki, K., and Yamaguchi-Shinozaki, K. (2005). AREB1 is a transcription activator of novel ABRE-dependent ABA signaling that enhances drought stress tolerance in *Arabidopsis*. Plant Cell **17:** 3470–3488.

Gill, U.S., Lee, S., and Mysore, K.S. (2015). Host versus nonhost resistance: distinct wars with similar arsenals. Phytopathology **105:** 580–587.

Golemis, E. (2002). Protein-Protein Interactions: A Molecular Cloning Manual. (New York: Cold Spring Harbor Laboratory Press).

Gudesblat, G.E., Torres, P.S., and Vojnov, A.A. (2009b). *Xanthomonas campestris* overcomes Arabidopsis stomatal innate immunity through a DSF cell-to-cell signal-regulated virulence factor. Plant Physiol. **149:** 1017–1027.

Hanson, P.I., and Whiteheart, S.W. (2005). AAA+ proteins: have engine, will work. Nat. Rev. Mol. Cell Biol. **6:** 519–529.

Heath, M.C. (1987). Evolution of plant resistance and susceptibility to fungal invaders. Can. J. Plant Pathol. **9:** 389–397.

Heath, M.C. (2000). Nonhost resistance and nonspecific plant defenses. Curr. Opin. Plant Biol. **3:** 315–319.

Herrmann, C., Horn, G., Spaargaren, M., and Wittinghofer, A. (1996). Differential interaction of the ras family GTP-binding proteins H-Ras, Rap1A, and R-Ras with the putative effector molecules Raf kinase and Ral-guanine nucleotide exchange factor. J. Biol. Chem. **271:** 6794–6800.

Ishiga, Y., Ishiga, T., Uppalapati, S.R., and Mysore, K.S. (2011). *Arabidopsis* seedling flood-inoculation technique: a rapid and reliable assay for studying plant-bacterial interactions. Plant Methods **7:** 32.

Jahn, T., Fuglsang, A.T., Olsson, A., Brüntrup, I.M., Collinge, D.B., Volkmann, D., Sommarin, M., Palmgren, M.G., and Larsson, C. (1997). The 14-3-3 protein interacts directly with the C-terminal region of the plant plasma membrane H^+-ATPase. Plant Cell **9:** 1805–1814.

Jefferson, R.A., Kavanagh, T.A., and Bevan, M.W. (1987). GUS fusions: β-glucuronidase as a sensitive and versatile gene fusion marker in higher plants. EMBO J. **6:** 3901–3907.

Jones, J.D., and Dangl, J.L. (2006). The plant immune system. Nature **444:** 323–329.

Kim, H.M., Yu, Y., and Cheng, Y. (2011). Structure characterization of the 26S proteasome. Biochim. Biophys. Acta **1809:** 67–79.

Kudla, J., and Bock, R. (2016). Lighting the way to protein-protein interactions: recommendations on best practices for bimolecular fluorescence complementation analyses. Plant Cell **28:** 1002–1008.

Lee, D., Bourdais, G., Yu, G., Robatzek, S., and Coaker, G. (2015). Phosphorylation of the plant immune regulator RPM1-INTERACTING PROTEIN4 enhances plant plasma membrane H^+-ATPase activity and inhibits flagellin-triggered immune responses in *Arabidopsis*. Plant Cell **27:** 2042–2056.

Lee, S., Yang, D.S., Uppalapati, S.R., Sumner, L.W., and Mysore, K.S. (2013). Suppression of plant defense responses by extracellular metabolites from *Pseudomonas syringae* pv. *tabaci* in *Nicotiana benthamiana*. BMC Plant Biol. **13:** 65.

Lim, C.W., Baek, W., Jung, J., Kim, J.-H., and Lee, S.C. (2015). Function of ABA in stomatal defense against biotic and drought stresses. Int. J. Mol. Sci. **16:** 15251–15270.

Liu, J., Elmore, J.M., Fuglsang, A.T., Palmgren, M.G., Staskawicz, B.J., and Coaker, G. (2009). RIN4 functions with plasma membrane H^+-ATPases to regulate stomatal apertures during pathogen attack. PLoS Biol. **7:** e1000139.

Lozano-Durán, R., Bourdais, G., He, S.Y., and Robatzek, S. (2014). The bacterial effector HopM1 suppresses PAMP-triggered oxidative burst and stomatal immunity. New Phytol. **202:** 259–269.

Mackey, D., Holt III, B.F., Wiig, A., and Dangl, J.L. (2002). RIN4 interacts with *Pseudomonas syringae* type III effector molecules and is required for RPM1-mediated resistance in *Arabidopsis*. Cell **108:** 743–754.

Maier, F., Zwicker, S., Hückelhoven, A., Meissner, M., Funk, J., Pfitzner, A.J.P., and Pfitzner, U.M. (2011). NONEXPRESSOR OF PATHOGENESIS-RELATED PROTEINS1 (NPR1) and some NPR1-related proteins are sensitive to salicylic acid. Mol. Plant Pathol. **12:** 73–91.

Mara, C., Grigorova, B., and Liu, Z. (2010). Floral-dip transformation of *Arabidopsis thaliana* to examine pTSO2:β-glucuronidase reporter gene expression. J. Vis. Exp. **40:** 1952.

Marre, E. (1979). Fusicoccin—tool in plant physiology. Annu. Rev. Plant Physiol. Plant Mol. Biol. **30:** 273–288.

McLachlan, D.H., Kopischke, M., and Robatzek, S. (2014). Gate control: guard cell regulation by microbial stress. New Phytol. **203:** 1049–1063.

Melotto, M., Underwood, W., Koczan, J., Nomura, K., and He, S.Y. (2006). Plant stomata function in innate immunity against bacterial invasion. Cell **126:** 969–980.

Meng, X., and Zhang, S. (2013). MAPK cascades in plant disease resistance signaling. Annu. Rev. Phytopathol. **51:** 245–266.

Merlot, S., Leonhardt, N., Fenzi, F., Valon, C., Costa, M., Piette, L., Vavasseur, A., Genty, B., Boivin, K., Müller, A., Giraudat, J., and Leung, J. (2007). Constitutive activation of a plasma membrane H^+-ATPase prevents abscisic acid-mediated stomatal closure. EMBO J. **26:** 3216–3226.

Misra, B.B., de Armas, E., Tong, Z., and Chen, S. (2015). Metabolomic responses of guard cells and mesophyll cells to bicarbonate. PLoS One **10:** e0144206.

Mysore, K.S., and Ryu, C.M. (2004). Nonhost resistance: how much do we know? Trends Plant Sci. **9:** 97–104.

Obulareddy, N., Panchal, S., and Melotto, M. (2013). Guard cell purification and RNA isolation suitable for high-throughput transcriptional analysis of cell-type responses to biotic stresses. Mol. Plant Microbe Interact. **26:** 844–849.

Ogura, T., Fujiki, Y., and Katayama, T. (2012). AAA+ proteins. J. Struct. Biol. **179:** 77.

Pant, B.D., Burgos, A., Pant, P., Cuadros-Inostroza, A., Willmitzer, L., and Scheible, W.R. (2015). The transcription factor PHR1 regulates lipid remodeling and triacylglycerol accumulation in *Arabidopsis thaliana* during phosphorus starvation. J. Exp. Bot. **66:** 1907–1918.

Rojas, C.M., Senthil-Kumar, M., Wang, K., Ryu, C.M., Kaundal, A., and Mysore, K.S. (2012). Glycolate oxidase modulates reactive oxygen species-mediated signal transduction during nonhost resistance in *Nicotiana benthamiana* and *Arabidopsis*. Plant Cell **24:** 336–352.

Ruijter, J.M., Ramakers, C., Hoogaars, W.M.H., Karlen, Y., Bakker, O., van den Hoff, M.J.B., and Moorman, A.F. (2009). Amplification efficiency: linking baseline and bias in the analysis of quantitative PCR data. Nucleic Acids Res. **37:** e45.

Senthil-Kumar, M., and Mysore, K.S. (2013). Nonhost resistance against bacterial pathogens: retrospectives and prospects. Annu. Rev. Phytopathol. **51:** 407–427.

Senthil-Kumar, M., and Mysore, K.S. (2014). Tobacco rattle virus-based virus-induced gene silencing in *Nicotiana benthamiana*. Nat. Protoc. **9:** 1549–1562.

Serebriiskii, I., Khazak, V., and Golemis, E.A. (1999). A two-hybrid dual bait system to discriminate specificity of protein interactions. J. Biol. Chem. **274:** 17080–17087.

Sirichandra, C., Gu, D., Hu, H.C., Davanture, M., Lee, S., Djaoui, M., Valot, B., Zivy, M., Leung, J., Merlot, S., and Kwak, J.M. (2009a). Phosphorylation of the *Arabidopsis* AtrbohF NADPH oxidase by OST1 protein kinase. FEBS Lett. **583:** 2982–2986.

Sirichandra, C., Wasilewska, A., Vlad, F., Valon, C., and Leung, J. (2009b). The guard cell as a single-cell model towards understanding drought tolerance and abscisic acid action. J. Exp. Bot. **60:** 1439–1463.

Sousa, R. (2014). Structural mechanisms of chaperone mediated protein disaggregation. Front. Mol. Biosci. **1:** 12.

Sugimoto, M., Yamaguchi, Y., Nakamura, K., Tatsumi, Y., and Sano, H. (2004). A hypersensitive response-induced ATPase associated with various cellular activities (AAA) protein from tobacco plants. Plant Mol. Biol. **56:** 973–985.

Underwood, W., Melotto, M., and He, S.Y. (2007). Role of plant stomata in bacterial invasion. Cell. Microbiol. **9:** 1621–1629.

Üstün, S., Bartetzko, V., and Börnke, F. (2015). The *Xanthomonas* effector XopJ triggers a conditional hypersensitive response upon treatment of *N. benthamiana* leaves with salicylic acid. Front. Plant Sci. **6:** 599.

Vierstra, R.D. (2009). The ubiquitin-26S proteasome system at the nexus of plant biology. Nat. Rev. Mol. Cell Biol. **10:** 385–397.

Wang, K., Kang, L., Anand, A., Lazarovits, G., and Mysore, K.S. (2007). Monitoring *in planta* bacterial infection at both cellular and whole-plant levels using the green fluorescent protein variant GFPuv. New Phytol. **174:** 212–223.

Wang, K., Senthil-Kumar, M., Ryu, C.M., Kang, L., and Mysore, K.S. (2012). Phytosterols play a key role in plant innate immunity against bacterial pathogens by regulating nutrient efflux into the apoplast. Plant Physiol. **158:** 1789–1802.

White, S.R., and Lauring, B. (2007). AAA+ ATPases: achieving diversity of function with conserved machinery. Traffic **8:** 1657–1667.

Wick, P., Gansel, X., Oulevey, C., Page, V., Studer, I., Dürst, M., and Sticher, L. (2003). The expression of the t-SNARE AtSNAP33 is induced by pathogens and mechanical stimulation. Plant Physiol. **132:** 343–351.

Yasuda, S., Sato, T., Maekawa, S., Aoyama, S., Fukao, Y., and Yamaguchi, J. (2014). Phosphorylation of *Arabidopsis* ubiquitin ligase ATL31 is critical for plant carbon/nitrogen nutrient balance response and controls the stability of 14-3-3 proteins. J. Biol. Chem. **289:** 15179–15193.

Zeng, W., and He, S.Y. (2010). A prominent role of the flagellin receptor FLAGELLIN-SENSING2 in mediating stomatal response to *Pseudomonas syringae* pv *tomato* DC3000 in Arabidopsis. Plant Physiol. **153:** 1188–1198.

Zhang, B., Karnik, R., Wang, Y., Wallmeroth, N., Blatt, M.R., and Grefen, C. (2015). The *Arabidopsis* R-SNARE VAMP721 interacts with KAT1 and KC1 K^+ channels to moderate K^+ current at the plasma membrane. Plant Cell **27:** 1697–1717.

Zhao, Z., Zhang, W., Stanley, B.A., and Assmann, S.M. (2008). Functional proteomics of *Arabidopsis thaliana* guard cells uncovers new stomatal signaling pathways. Plant Cell **20:** 3210–3226.

Zhou, Z., Wu, Y., Yang, Y., Du, M., Zhang, X., Guo, Y., Li, C., and Zhou, J.M. (2015). An *Arabidopsis* plasma membrane proton ATPase modulates JA signaling and is exploited by the *Pseudomonas syringae* effector protein AvrB for stomatal invasion. Plant Cell **27:** 2032–2041.

GENERAL CONTROL NONREPRESSIBLE4 Degrades 14-3-3 and the RIN4 Complex to Regulate Stomatal Aperture with Implications on Nonhost Disease Resistance and Drought Tolerance

Amita Kaundal, Vemanna S. Ramu, Sunhee Oh, Seonghee Lee, Bikram Pant, Hee-Kyung Lee, Clemencia M. Rojas, Muthappa Senthil-Kumar and Kirankumar S. Mysore

Plant Cell 2017;29;2233-2248; originally published online August 30, 2017;
DOI 10.1105/tpc.17.00070